

T 1406

GEOLOGY OF THE HAYDEN PASS--ORIENT MINE AREA,
NORTHERN SANGRE DE CRISTO MOUNTAINS, COLORADO:
A GEOLOGIC REMOTE SENSING EVALUATION

By

Daniel C. Wychgram

ProQuest Number:10781745

All rights reserved

INFORMATION TO ALL USERS

The quality of this reproduction is dependent upon the quality of the copy submitted.

In the unlikely event that the author did not send a complete manuscript and there are missing pages, these will be noted. Also, if material had to be removed, a note will indicate the deletion.



ProQuest 10781745

Published by ProQuest LLC (2018). Copyright of the Dissertation is held by the Author.

All rights reserved.

This work is protected against unauthorized copying under Title 17, United States Code
Microform Edition © ProQuest LLC.

ProQuest LLC.
789 East Eisenhower Parkway
P.O. Box 1346
Ann Arbor, MI 48106 – 1346

A Thesis submitted to the Faculty and the Board of Trustees of the Colorado School of Mines in partial fulfillment of the requirements for the degree of Master of Science (Geology).

Signed: Daniel C. Wychgram
Daniel C. Wychgram

Golden, Colorado

Date: February 21, 1972

ARTHUR LAKES LIBRARY
COLORADO SCHOOL OF MINES
GOLDEN, COLORADO

Approved: Keenan Lee
Keenan Lee
Thesis Advisor

Harry C. Kent
Harry C. Kent
Department Head

Golden, Colorado

Date: March 6, 1972

ABSTRACT

The Hayden Pass--Orient Mine area includes 60 square miles of the northern Sangre de Cristo Mountains and San Luis Valley in south-central Colorado. The study of this area consists of two parts; (1) description and interpretation of the stratigraphy, structure, and geologic history of the area, and (2) research into the application of remote sensor data to the geologic problems of the area.

The rocks of the Hayden Pass--Orient Mine area include Precambrian igneous and metamorphic rocks, Paleozoic sedimentary rocks, Tertiary intrusive rocks, and Quaternary deposits. Lower and middle Paleozoic rocks consist of about 1,000 feet of limestone, dolomite, and quartzite deposited in a stable shelf environment which was interrupted by minor, periodic episodes of uplift and erosion. A very thick (over 9,000 feet) sequence of upper Paleozoic rocks includes light gray and tan, quartzose sandstones and interbedded shales (Kerber Formation); red micaceous, and arkosic sandstones, siltstones, and shale (Sharpsdale Formation); grayish-green, feldspathic, conglomerates and sandstones with interbedded shales (Minturn Formation); and red, arkosic, pebble

conglomerates and sandstones with interbedded siltstones and shales (Sangre de Cristo Formation). These rocks were deposited in continental, transitional, and shallow marine environments of the Central Colorado trough. During early Tertiary, a stock (herein informally named the Slide Rock Mountain Intrusive) was intruded in the northeastern part of the area. Quaternary deposits include pediment gravels and glacial deposits. Coalescing alluvial fans of the San Luis Valley have been subdivided into four fan units based on geomorphology and vegetation. The age relationships of these fan units have been established by physical criteria such as degree of dissection and truncation of fan surface drainage.

The Hayden Pass--Orient Mine area has been affected by three major episodes of tectonic activity. The Pennsylvanian and Permian Ancestral Rocky Mountain orogeny, dominated by subvertical faulting, produced the Ancestral Rocky highlands and Central Colorado trough. Beginning in Late Cretaceous, the Laramide orogeny produced many northwest-trending folds and reverse faults in the area. The compressional stresses of the Laramide orogeny subsided during the Eocene. By Miocene time, a third major tectonic episode had begun. This taphrogenic post-Laramide tectonic activity has formed the Rio Grande Rift Zone, of which the San Luis Valley is a part. The area is currently under the influence of this episode of extensional tectonics.

Remote sensor data from a NASA Convair 990 radar flight and Missions 101 and 105 have been interpreted and evaluated. Based on interpretation of the remote sensor data, a geologic map (Plate II) has been prepared and compared with a second geologic map (Plate I), prepared from interpretation of both remote sensor data and field data. Comparison of the two maps gives one indication of the usefulness and reliability of the remote sensor data.

The usefulness and reliability of the remote sensor data are a function of the type of terrain as well as the type of remote sensor used. The San Luis Valley, with low relief and sparse vegetation, proved to be the best area to apply remote sensing. The western slope of the mountains is less suitable to the use of remote sensing techniques because of the dense coniferous cover and high relief. The eastern slope of the mountains, which is very densely covered with conifers and has high relief, is least suited to the use of remote sensing.

By using remote sensing as an aid in mapping the geologic features of the area, advantages were realized over purely field methods. These advantages include time savings, a greater understanding of certain geological phenomena, and the compilation of a more accurate and complete geologic map.

Color and color infrared photography provided the largest amount of valuable information. Multiband photography was of lesser value and side-looking radar imagery provided no new information that was not available on small-scale photography.

Thermal scanner imagery proved to be a very specialized remote sensing tool that should be applied to areas of low relief and sparse vegetation where geologic features produce known or suspected thermal contrast. Low sun-angle photography may be a good alternative to side-looking radar imagery but must be flown with critical timing.

CONTENTS

	Page
Abstract	iii
Introduction	1
Location and Physiography	1
Previous Investigations	4
Purpose	7
Acknowledgments	8
Stratigraphy	10
Precambrian Rocks	10
Paleozoic Rocks	13
Pre-Pennsylvanian Rocks	13
Ordovician	14
Manitou Dolomite	14
Harding Sandstone	14
Fremont Dolomite	14
Devonian	15
Chaffee Formation	15
Mississippian	16
Leadville Limestone	16
Pennsylvanian and Permian Rocks	17
Kerber Formation	19
Sharpsdale Formation	21
Minturn Formation	21
Sangre de Cristo Formation	29
Mesozoic Rocks	32
Cenozoic Rocks	33
Tertiary Intrusives and Volcanic Rocks	33
Slide Rock Mountain Intrusive	33
Igneous Dikes	36
Volcanic Rocks	37
Quaternary Deposits	38
Glacial Deposits	38
Pediment Gravels	38
San Luis Valley Alluvial Fans	42

	Page
Structural Geology	44
Folding	46
Folds on the West Slope	46
Folds on the East Slope	48
Faulting	50
Hypothetical and Inferred Faults of Unknown Geometry	50
Reverse Faults Near the Arkansas Valley	53
Longitudinal Faults Related to Folding on the West Slope	55
Transverse Faults on the West Slope	57
Normal Faults in the San Luis Valley	57
Structural History	60
Ancestral Rocky Mountain Orogeny	61
Laramide Orogeny	61
Post-Laramide Tectonics--Taphrogeny	63
Geologic History	65
Applications of Remote Sensing Methods to Geologic Problems	73
Description of Test Site	74
San Luis Valley--Area 'A'	75
West Flank of the Sangre de Cristo Mountains--Area 'B'	78
East Flank of the Sangre de Cristo Mountains--Area 'C'	81
Data Collection	82
NASA Convair 990 Radar Flight	83
NASA Mission 101	84
NASA Mission 105	84
Interpretation and Evaluation of Remote Sensor Data	89
Schedule and Method	89
Convair 990 Radar Flight	91
Mission 101	93
Mission 105	98
Recent Supplementary Data--Mission 168	110
Conclusions	117
Bibliography	124

ILLUSTRATIONS

Figure	Page
1. Index map of Hayden Pass--Orient Mine area	2
2. Thesis area as viewed from the San Luis Valley	5
3. Index map to previous geologic work in the vicinity of the Hayden Pass--Orient Mine area	6
4. Summary stratigraphic column	11
5. Pennsylvanian geomorphic elements in south-central Colorado	20
6. Photomicrograph of sandstone in Sharpsdale Formation showing graded bedding	22
7. Tabular cross-bedding in the Minturn Formation	25
8. Photomicrograph of crinoidal packstone of Unit I.	27
9. Photomicrograph of biotite-quartz monzonite of Slide Rock Mountain Intrusive	34
10. Photomicrograph of quartz-lattice porphyry of a dike located on the crest of the range	34
11. Cirque on north side of Nipple Mountain	39
12. Areal distribution of calcite-cemented pediment gravels	41
13. Regional tectonic features of south-central Colorado	45
14. Steel Canyon anticline and overturned Steel Canyon syncline	47
15. Fault, gouge, and disrupted bedding zone on northeast side of a major inferred fault	52

Figure	Page
16. Eroded fault scarp in the San Luis Valley	76
17. Hypothetical cross section of a typical fault in the San Luis Valley	79
18. Reproduction of Venus Fly-by radar imagery . . .	92
19a. Annotated reproduction of Mission 101 color photography	95
19b. Unannotated reproduction of Mission 101 color photography	95
20. Geologic map based on interpretation of Mission 101 color and color IR photography	97
21a. Annotated reproduction of Mission 105 color photography	99
21b. Unannotated reproduction of Mission 105 color photography	99
22a. Annotated reproduction of RS-14 thermal infrared scanner imagery	108
22b. Unannotated reproduction of RS-14 thermal infrared scanner imagery	108
23a. Low sun-angle photography of fault scarps in San Luis Valley	113
23b. Low sun-angle photography of fault scarps in San Luis Valley taken 16 minutes after Figure 23a	113
24. Forest Service photograph showing location of temperature monitoring stations	115
25. Reproduction of Mission 168 thermal infrared imagery	115
 Plate	
I. Geologic map and cross sections, Hayden Pass-- Orient Mine area, Saguache, Custer, and Fremont Counties, Colorado	Pocket
II. Geologic map based on remote sensor data--Map A; Map showing division of area into three subareas-- Map B	Pocket

TABLES

Table	Page
1. Nomenclature history of Pennsylvanian and Permian rocks, northern Sangre de Cristo Range	18
2. NASA Convair 990 radar flight--flown May 19, 1969	83
3. NASA Mission 101--flown August 11-12, 1969	85
4. NASA Mission 105--flown October 2, 1969	86
5. Formational characteristics of Paleozoic and Precambrian rocks of Area 'B' that are apparent on Mission 105 color photography	104
6. Summary of remote sensing instrument and data parameters--Mission 168	111
7. Measurements on fault scarps in San Luis Valley, June 16, 1971	116

INTRODUCTION

This research has produced essentially two theses under one title. The first thesis is concerned with the detailed field mapping and interpretation of the stratigraphy, structure, and geologic history of the Hayden Pass--Orient Mine area. The second thesis concerns research into the application of remote sensor data to the geologic problems of this same area.

It is realized that the reader may have a particular interest in only one of these topics. With this consideration in mind, both sections have been written so that they may be read independently. The stratigraphy, structure, and geologic history of the area are presented first, followed by the application of remote sensing methods.

Location and Physiography

The Hayden Pass--Orient Mine area is in the rugged northern Sangre de Cristo Mountains, 25 miles southeast of Salida, Colorado (Figure 1). The area mapped includes approximately 60 square miles, extending from San Luis Creek on the southwest to the Arkansas River on the northeast, and from Hayden Pass Road on the northwest to the

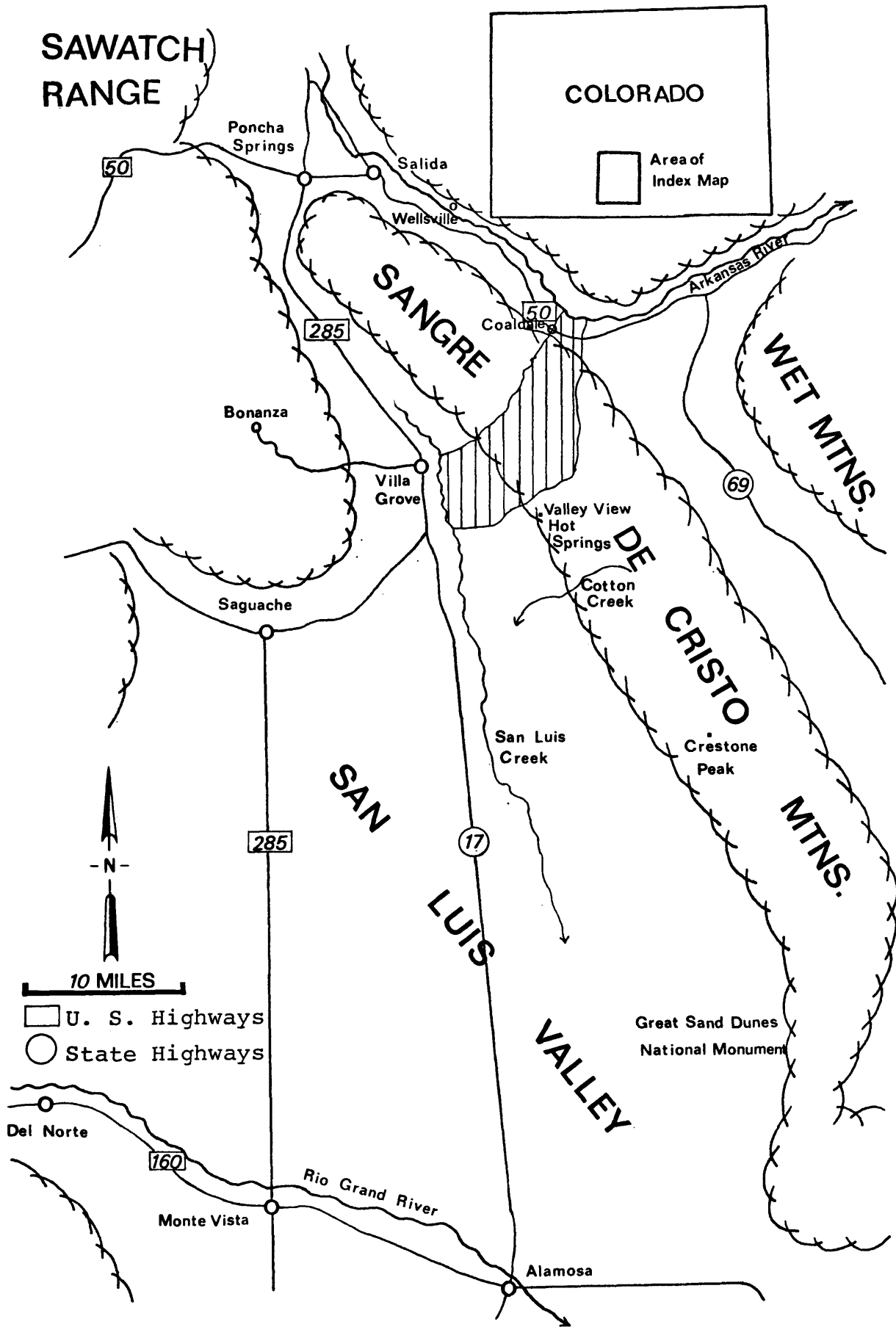


Figure 1. Index map of Hayden Pass--Orient Mine area (lined).

Big Cottonwood Creek and Black Canyon drainage systems on the southeast. The area includes parts of Rio Grande National Forest and Saguache County on the west side of the range crest and parts of San Isabel National Forest, Custer and Fremont counties, on the east side of the crest.

The area is accessible from Hayden Pass Road, which borders the area to the northwest, and which extends from a junction with U. S. Highway 285 at Villa Grove in the San Luis Valley to a junction with U. S. Highway 50 at Coaldale near the Arkansas River. Most of the road is recommended for four-wheel-drive vehicles only. Rough jeep trails exist in Steel and Black canyons on the west, and in the Pole Gulch and the Big Cottonwood Creek drainage areas on the east. None of these trails extends to within 2 miles of the crest of the range.

The Sangre de Cristo Range, one of the most spectacular ranges in Colorado, is characterized by its narrow width, high relief, and asymmetry. The peaks along the crest average more than 12,000 feet in elevation, and the relief between the Arkansas River at Coaldale and Nipple Mountain (12,199 feet) is almost 6,000 feet. The width of the range from the crest to its base in the San Luis Valley is only about 2 miles, whereas the width from the crest to the Arkansas River valley is about 6 miles. The sharply defined

crest of the range, most of which is above timberline, is modified by alpine glacial features. The east side of the range is drained by tributaries of the Arkansas River. On the west side of the range, most of the runoff sinks into alluvial fans of the San Luis Valley near the base of the mountains.

Figure 2 shows the thesis area as viewed from a distance of 8 miles in the San Luis Valley. Hayden Pass, the lowest point in the range crest, is seen on the left. Just right of center is Nipple Mountain with its characteristic profile. Cottonwood Peak, which is to the southeast of the mapped area, is just out of the picture to the right. As can be seen in the photograph, the area has a thick cover of conifers.

Previous Investigations

The region was first examined geologically, on a reconnaissance basis, by Endlich (1874). Johnson (1929, 1945) discussed the stratigraphy of parts of the range and has contributed much to the Paleozoic stratigraphy of Colorado. In addition, regional contributions have been made by Burbank and Goddard (1937) and Gabelman (1952).

The northern Sangre de Cristo Mountains have received considerable attention within the past 15 years from geologists working on advanced degrees. Figure 3 shows the locations of previous geologic work done in and near the Hayden Pass--Orient Mine area. The work of Litsey (1954)

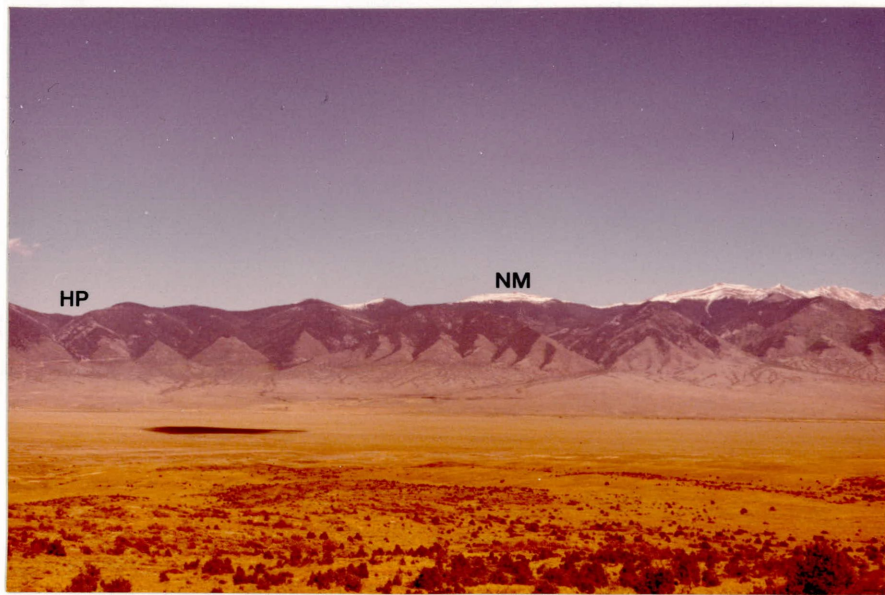


Figure 2. Thesis area as viewed from the San Luis Valley, 8 miles southwest of the mountain front. Hayden Pass (HP) and Nipple Mountain (NM) can be seen on the skyline.

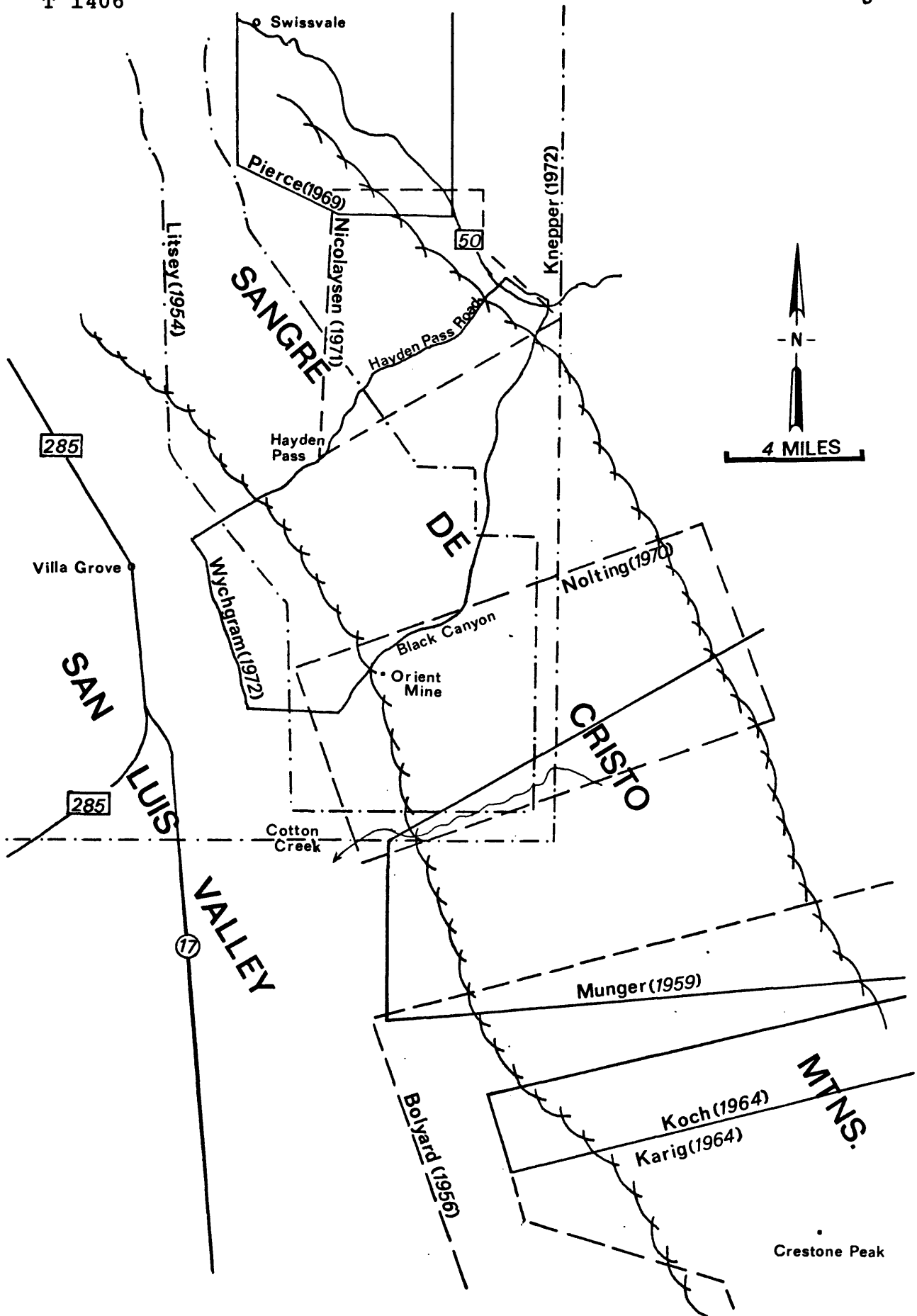


Figure 3. Index map to previous geologic work in the vicinity of the Hayden Pass--Orient Mine area.

is of particular significance. He mapped the structure and stratigraphy of the northern Sangre de Cristo Mountains from Wellsville south to Cotton Creek, with emphasis on the rocks of early and middle Paleozoic age. Important recent contributions have come from Pierce (1969), Nolting (1970), and Peel (1971). Pierce has done a detailed stratigraphic study of the Pennsylvanian and Permian rocks in the vicinity of the Arkansas River near Swissvale. Nolting's work includes detailed mapping of the structure and stratigraphy of the range immediately southeast of the Hayden Pass--Orient Mine area. Peel has dealt with Pennsylvanian and Permian stratigraphy and structural history on a regional basis, which includes most of the area discussed in this thesis. Nicolaysen (1971) has recently finished detailed mapping in the vicinity of Hayden Pass Road and to the northwest. Knepper (1972) is doing a regional study of the Rio Grande rift zone and has included the area between Hayden Pass and the Orient Mine in his synthesis.

Purpose

The area between Hayden Pass Road and the Orient Mine represented one of the last links in a chain of detailed geologic mapping in the northern Sangre de Cristo Range (Figure 3). Nicolaysen has extended Pierce's work south to the vicinity of Hayden Pass Road, and Nolting, Munger (1959), Bolyard (1956), Koch (1964), Karig (1964), and

others have extended detailed mapping from Crestone Peak north to Black Canyon. A purpose of this study was to contribute to the completion of this chain of detailed mapping.

A second purpose of the study was to interpret and to evaluate Bonanza Project remote sensor data and to determine the potential of the various remote sensor systems as applied to geologic problems. The Bonanza Project test site includes the northern Sangre de Cristo Range, and a limited amount of remote sensor data on the Hayden Pass--Orient Mine area was already available (see Tables 2, 3, and 4). The thesis area is particularly well suited to the evaluation of remote sensor data because it encompasses two markedly different terrains, which provide remote sensor target variations concerning geology, hydrology, vegetation, and topography.

Acknowledgments

I am indebted to the Bonanza Remote Sensing Project, sponsored by the National Aeronautics and Space Administration (Grant NGL 06-001-015), which has provided financial support in the form of a Research Assistantship from February 1970 through August 1971 and the remote sensor data upon which much of this thesis is based. Furthermore, experience and knowledge gained in the planning and ground control activities of remote sensing missions and in course work related to the Project have

greatly enhanced my ability to interpret the data used in this thesis.

Appreciation is expressed to the people of Martin Marietta Corporation's Interplanetary Geology Lab, especially to Messrs. Jim Muhm, Ken Worman, Roland Hulstrom, and Bob Biniki for help and advice.

I wish to thank Professors Keenan Lee, L. Trowbridge Grose, and Richard H. De Voto for advice and constructive criticism during field trips and meetings.

Finally, I wish to express sincere thanks to my wife, Virginia, for working with me for months in both the field and office as field assistant and secretary.

STRATIGRAPHY

The rocks within the thesis area include Precambrian igneous and metamorphic rocks, Paleozoic sedimentary rocks, Tertiary intrusive rocks, and Quaternary deposits of several origins. It is convenient to subdivide the Paleozoic rocks into "pre-Pennsylvanian" and "Pennsylvanian and Permian" based on the striking differences which occur in lithology, thickness, and inferred environment of deposition.

The terminology used in this thesis is in keeping with the latest work done in the surrounding area. Pennsylvanian and Permian stratigraphic nomenclature has been adopted from Peel (1971), De Voto and others (1971) and De Voto (1971, written communication) as further explained in that section. Classification and nomenclature for Quaternary deposits in the San Luis Valley are the same as those used by Knepper (1972). A summary stratigraphic column is presented in Figure 4.

Precambrian Rocks

Precambrian rocks are exposed in a narrow strip, one-half to one mile wide, on the west flank of the mountains along the San Luis Valley. The thesis area is bounded by Precambrian rocks to the northeast across the Arkansas River

Summary Description

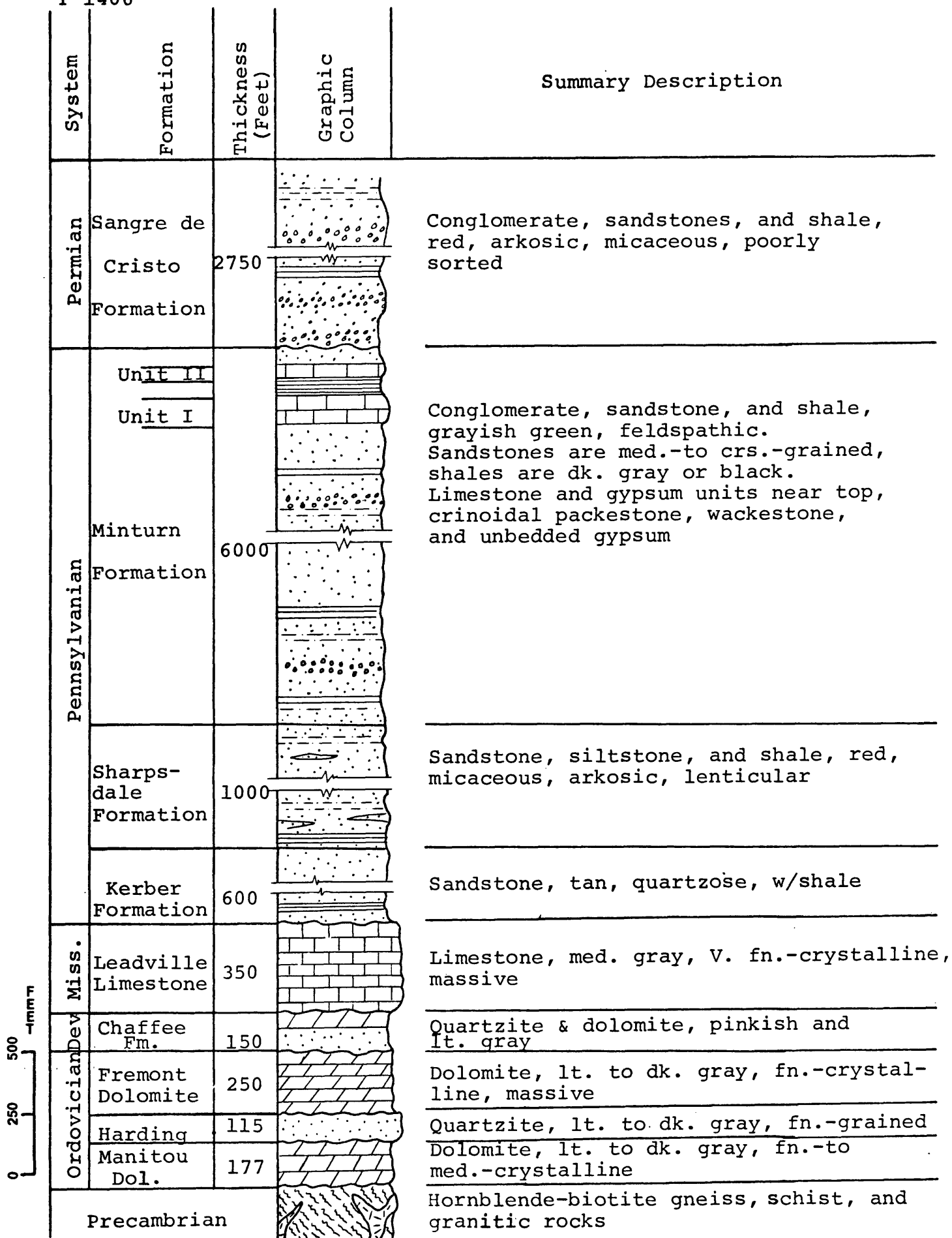


Figure 4. Summary stratigraphic column.

and to the east in the lower reaches of Big Cottonwood Creek (Plate I). No attempt was made to map the various lithologic units or to study the structural features of these rocks.

Generally, the crystalline rocks on the west flank of the range are hornblende-biotite gneiss with some schist occurring locally and several intrusions of fine-to medium-grained granite and monzonite. Foliation has a general northerly strike, and dips which are steep or vertical. The foliation is often so prominent as to be mistaken for sedimentary bedding on aerial photographs.

Northeast of the Arkansas River and east of lower Big Cottonwood Creek, the Precambrian rocks are generally granitic and of two types. A pink, coarse-grained granite is the dominant rock type with a fine-to medium-grained, gray granite being less prevalent. A more mafic constituent, possibly occurring as xenoliths, was also noted. Gabelman (1952) cites these granitic rocks as being Pikes Peak Granite and Silver Plume Granite equivalents respectively.

The contact between the Precambrian crystalline rocks of the west flank of the mountains and the overlying Manitou Dolomite was not observed in outcrop. However, Nolting (1970, p. 9) reports this contact to be a nonconformity with about 2 feet of relief. A probable fault contact exists

between the crystalline and sedimentary rocks in the north-eastern part of the thesis area.

Paleozoic Rocks

Pre-Pennsylvanian Rocks

The pre-Pennsylvanian sedimentary rocks are relatively thin units consisting mainly of dolomite and limestone with lesser amounts of quartzite and sandstone. Disconformities exist between most of the formations. A stable shelf environment with minor, periodic uplift is indicated during this period of deposition.

Litsey (1954) has made a more detailed study of the stratigraphy of the lower and middle Paleozoic rocks extending from Wellsville to south of the thesis area. The following is a brief description of the lithologic units.

Although no rocks of Cambrian age occur in the thesis area, Litsey (1958, p. 1149) states that the Sawatch Sandstone of late Cambrian age occurs in isolated places near the Sangre de Cristo Range. Bridwell (1968, p. 11) also described small amounts of Sawatch Sandstone in the Kerber Creek area, just across the San Luis Valley from the Hayden Pass--Orient Mine area. The Sawatch Sandstone probably once covered the entire region and was removed by pre-Ordovician erosion (Gabelman, 1952, p. 1582).

Ordovician

Manitou Dolomite: The Manitou Dolomite is a light to dark gray, locally reddish, medium to massive bedded, fine-to medium-crystalline dolomite. Locally black and white nodular and bedded chert is abundant. The formation weathers a characteristic brown and is 177 feet thick. Based on fossils collected from the formation, Johnson (1945, p. 18) indicates an Early Ordovician age for the Manitou Dolomite.

Harding Sandstone: The Harding Sandstone is a light to dark gray, fine-grained, medium-to thick-bedded, extremely hard quartzite. Locally, it is white banded or spotted. About 10 feet of red shale and siltstone occur near the base. The formation is 115 feet thick and Middle Ordovician in age (Litsey, 1958). The formation is reputed to have fish plates near its top (Litsey, 1958, p. 1153; Johnson, 1945, p. 21-22). The contact between the Manitou Dolomite and Harding Sandstone was in all cases concealed in the thesis area and its exact nature is not certain. Gabelman (1952, p. 1582) states that the contact is conformable, but Litsey (1958, p. 1153) cites thickness changes of the Manitou and the abrupt change in lithology between the two formations as evidence for a disconformity.

Fremont Dolomite: The Upper Ordovician Fremont Dolomite is a light to dark gray, fine-crystalline, thick-to massive-bedded dolomite. Its weathered surface is usually medium gray and

has a rough texture. This formation is easily confused with the Leadville Limestone but the difference in minerology can be used to differentiate them. The Fremont is quite fossiliferous with chain corals (possibly Halysites), tetracorals, and some poorly preserved brachiopods being found in abundance at certain localities. Litsey (1958, p. 1154) observed the contact between the Harding Sandstone and Fremont Dolomite to be undulatory near Galena Peak and suggests it may be a disconformity. The formation is about 250 feet thick.

Devonian

Chaffee Formation: The Chaffee Formation is often divided into the Parting Quartzite Member and the Dyer Dolomite Member. The Parting Quartzite Member is a white to pinkish conglomeratic quartzite with some shale near the base. The Dyer Dolomite Member is a pinkish to light gray, fine-crystalline, massive, dolomitic limestone which weathers a characteristic yellow. Division of the formation into its two members was found to be impractical for mapping purposes in the thesis area. The thickness of the formation is 150 feet and the age as given by Litsey (1958, p. 1156) is Late Devonian. Although the contact between the Chaffee Formation and the Fremont Dolomite was not observed, it is a well-documented disconformity (Litsey, 1954; Gabelman, 1952, p. 1583).

Mississippian

Leadville Limestone: The Leadville Limestone comprises 300 to 350 feet of light to medium gray, very fine-crystalline, massive limestone which weathers to a light gray or blue. The formation often contains black chert, white calcite veins and intraformational breccias. An unconformity exists between the Chaffee and Leadville formations (Litsey, 1958, p. 1155), although this relationship is difficult to observe in the field. The Leadville is very resistant and is an excellent marker unit to use in unraveling the complex structure of the western flank of the mountains. Many prospect pits were found in this formation with occasional shows of hematite, malachite, and azurite. The Orient Mine, located just south of Black Canyon, has produced over \$100,000 worth of iron ore (probably siderite) from the lower part of the Leadville Limestone (Litsey, 1960, p. 129). Although no fossils were found in the thesis area, Litsey (1954) and Johnson (1945) have determined that the formation is of Early Mississippian age.

Pennsylvanian and Permian Rocks

Permo-Pennsylvanian sedimentary rocks consist of a very thick sequence of coarse, generally arkosic, clastic rocks. This sequence has caused a great deal of confusion in terms of stratigraphic nomenclature and correlation. Correlation is made difficult by lithologies that vary greatly both vertically and horizontally and by complex folding and faulting. Recent investigators, notably Pierce (1969), Nolting (1970), and Peel (1971), have done much to alleviate this confusion. Pierce and Nolting, working north and south of the mapped area, respectively (see Figure 3), have done detailed stratigraphic work. Having excellent exposures, Pierce was able to subdivide the Pennsylvanian and Permian strata into seven well described units, primarily on the basis of color. Rather than correlating his rock units with established formations in other areas, Pierce designated them Unit I through Unit VII. Peel, using Pierce's basic units as a framework, was able to correlate them with rocks over a large area of the northern Sangre de Cristo Range (Table 1). The Permo-Pennsylvanian nomenclature and formational boundaries, as suggested by Peel and DeVoto (1972), have been adopted for use in this thesis.

The Hayden Pass--Orient Mine area is located within the Central Colorado trough which existed during deposition of Pennsylvanian and Permian sediments. Previous workers

System		Series		This Thesis		Peel & De Voto 1972		Peel 1971		Nolting 1970		Pierce 1969		Bolyard 1959		Brill 1952	
Permian		Wolfcampian		Sangre de Cristo Formation		upper member		upper member		Red Unit		Unit VII		Crestone Congl. Member		Sangre de Cristo Formation	
						lower member		lower member		Unit VI		Lower Member		Unit V		Lower Member	
Pennsylvanian		Desmoinesian		Minturn Formation		upper member		upper member		Green Unit		Unit III		Whiskey Cr. Pass Ls.		Minturn Formation	
						lower member		lower member		Unit IV		Whiskey Cr. Pass Ls.		Unit II		Deer Creek Formation	
Atokan		Morrowan		Sharpdale Formation		upper member		upper member		Maroon Unit		Unit I		Deer Creek Formation		Kerber Formation	
						lower member		lower member		Orange Unit		Unit II		Kerber Formation		Kerber Formation	
Permian		Wolfcampian		Sangre de Cristo Formation		upper member		upper member		Gray Unit		Unit I		Kerber Formation		Kerber Formation	
						lower member		lower member		Unit VI		Lower Member		Unit V		Lower Member	
Pennsylvanian		Desmoinesian		Minturn Formation		upper member		upper member		Green Unit		Unit III		Whiskey Cr. Pass Ls.		Minturn Formation	
						lower member		lower member		Unit IV		Whiskey Cr. Pass Ls.		Unit II		Deer Creek Formation	
Atokan		Morrowan		Sharpdale Formation		upper member		upper member		Maroon Unit		Unit I		Deer Creek Formation		Kerber Formation	
						lower member		lower member		Orange Unit		Unit II		Kerber Formation		Kerber Formation	

Table 1. Nomenclature history of Pennsylvanian and Permian rocks, northern Sangre de Cristo Range.

(De Voto, 1965; Nolting, 1970; Peel, 1971) have suggested that the depositional basin was probably narrow in this area. The relationship of the thesis area to the Uncompahgre highland, the Front Range highland, and the Central Colorado trough is shown in Figure 5.

Kerber Formation

The Kerber Formation rests unconformably on the Leadville Limestone. This irregular contact is well exposed at the Orient Mine where it is described by Litsey (1954, p. 50). Typical Kerber lithology is light gray, tan or buff, quartzose sandstones with a few thin, interbedded, buff to brown shales. Thin coal beds have been reported in this unit (Burbank, 1933, p. 13; Brill, 1952; Pierce, 1969), however, none was observed during field work. The Kerber Formation varies in thickness from about 400 to 600 feet. Accurate measurement of the unit is difficult because of complex structure and its gradational contact with the overlying Sharpsdale Formation. Although Bolyard (1960, p. 122) cites the sporadic occurrence of the Kerber Formation as evidence for erosion of this unit from much of south-central Colorado, it was found to be stratigraphically continuous throughout the thesis area. Also, the intertonguing nature of the contact between the Kerber Formation and the overlying Sharpsdale Formation

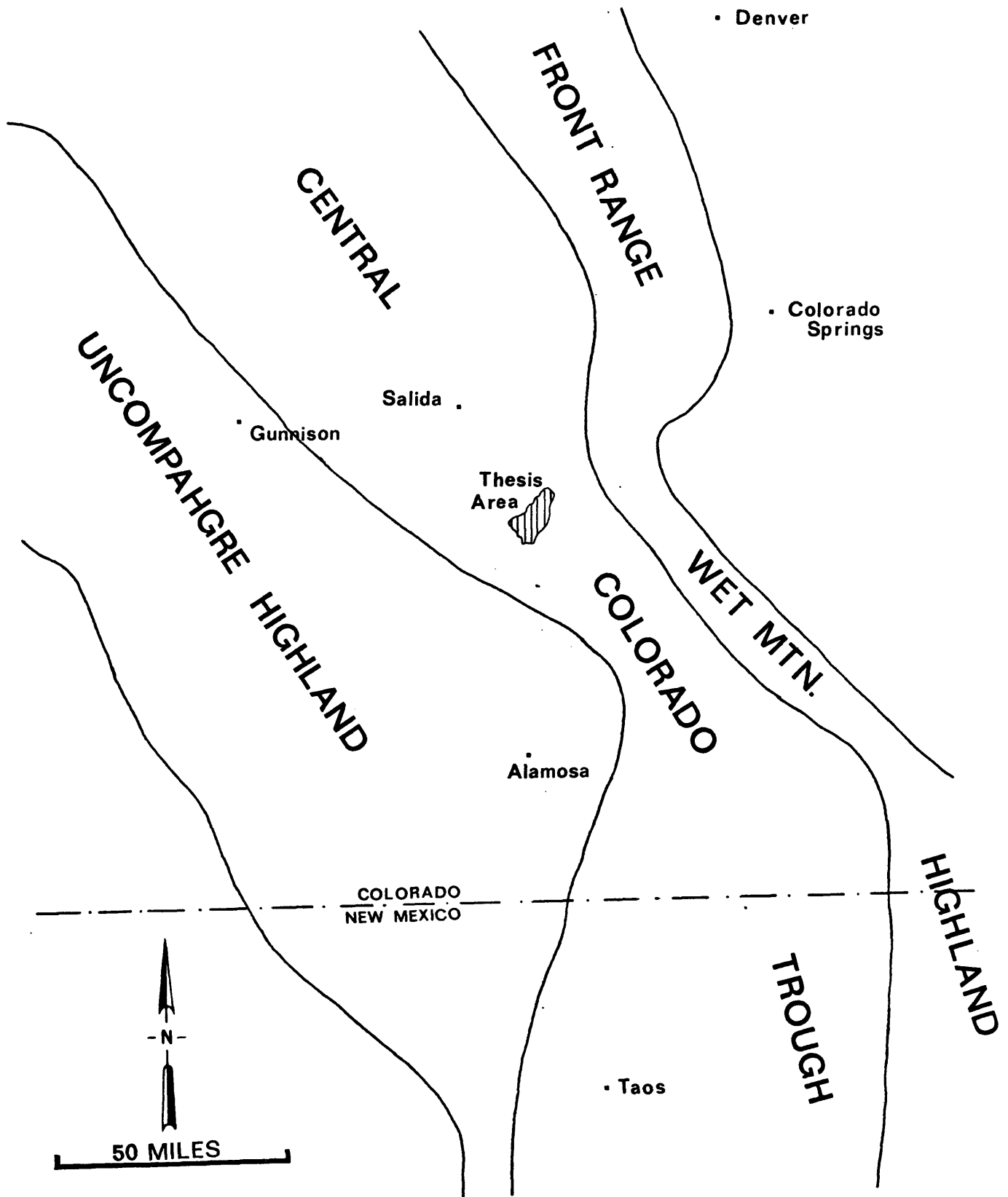


Figure 5. Pennsylvanian geomorphic elements in south-central Colorado (modified from Brill, 1952, Plate 3).

suggests that erosion was not significant in this area. The contact is placed where gray and buff quartzose beds of Kerber lithology give way to beds of red arkosic Sharpsdale lithology. The age of the Kerber Formation is not certain, but based on fossils found in the Sharpsdale Formation, Brill (1952, p. 815) suggests that the Kerber is Morrowan or Atokan.

Sharpsdale Formation

The Sharpsdale Formation consists of red, micaceous, and arkosic sandstones, siltstones, and shales. Some conglomeratic strata are also present. The sandstones are generally lenticular, poorly sorted, and often display graded bedding (see Figure 6), cross bedding, and cut-and-fill features. The matrix of the Sharpsdale is usually mud and clay with hematite and calcite cement. The thickness of this formation is estimated to be from 700 to 1,000 feet in the mapped area. Excellent exposures of Sharpsdale lithologies exist just south of Hayden Pass and just east of the Pass along Hayden Pass Road. Brill (1952, p. 830) has given an age of late Atokan to the Sharpsdale based on fossils found in Huerfano Park. The contact between the Sharpsdale Formation and the overlying Minturn Formation is gradational.

Minturn Formation

The Minturn Formation, which conformably overlies the Sharpsdale Formation, is 5,000 to 6,000 feet thick in the thesis area.

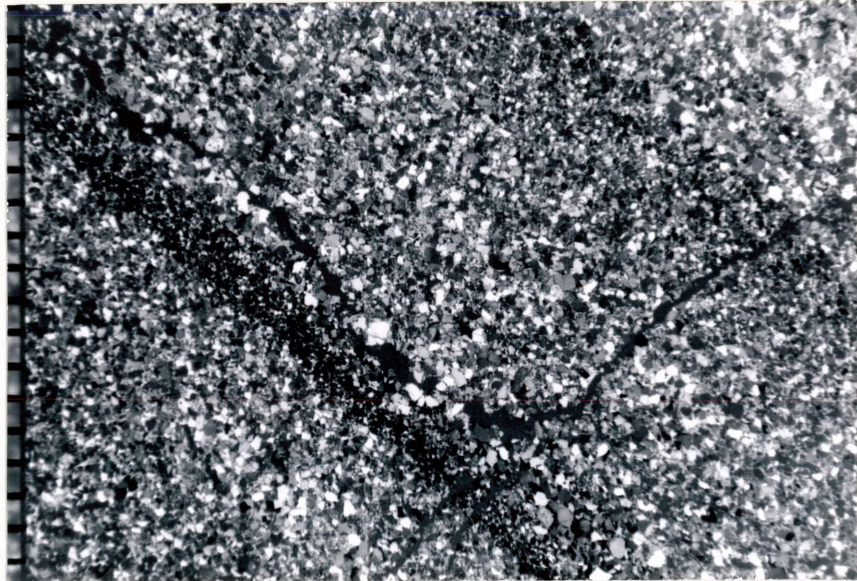


Figure 6. Photomicrograph of sandstone in Sharpsdale Formation showing graded bedding. Dark bands are hematite. Scale in millimeters. Sample was collected 300 yards southeast of Hayden Pass.

Precise measurement is impossible due to the complex structure that has disrupted this unit. Pierce (1969) reports about 1,200 feet stratigraphic thickness for his Unit III, the Minturn Formation. Peel (1971, p. 64) attributes this radical change in thickness to active fault displacement during the Pennsylvanian. Northwest-trending faults have been mapped that parallel the Arkansas River in the vicinity of the great thickness change. The Minturn Formation is time equivalent to the Madera Formation, and has been referred to by both names by previous workers (see Table 1). De Voto (1972) has recently redefined the Minturn Formation "to comprise the dominantly gray and green shales, siltstones, limestones, and sandstones occurring stratigraphically above the Belden, Sharpsdale, and Coffman Formations and below the Maroon and Sangre de Cristo Formations". The lithologies found in the Minturn Formation are varied but generally consist of gray, buff, and grayish-green pebble conglomerates and sandstones with some gray and black shales. The conglomerates are usually made up of pink granite or white quartz pebbles cemented in a green sandstone matrix. The sandstones are typically feldspathic, medium-to coarse-grained and have a green color which is characteristic of the formation. Based on thin-section

study, Walker (1967, p. 366) attributes the green color to interstitial chlorite. Shales are not as common as the conglomerates and sandstones and are usually finely bedded and interbedded with some sandstone. Cross bedding and ripple marks were often observed (see Figure 7). Good exposures of Minturn lithologies exist on Wolf Creek and along parts of Hayden Pass Road.

Near the top of the Minturn Formation is a sequence of interbedded limestones, gypsum, dark shales, and gray-green and buff sandstones. These lithologies are believed to be equivalent to the Unit D of Litsey (1958, p. 1160), and are probably related to Units IV, V, and VI of Nolting (1970, p. 33-39, Plate I).

Within the thesis area, the two dominant limestone-gypsum units of the sequence were mapped as "Unit I" and "Unit II" rather than mapping the entire sequence as one unit. This was done for two reasons. First, by mapping the limestone-gypsum units separately, more detail of the complex structural relationships could be represented and understood on the geologic map and cross-sections. Secondly, the clastic rocks of the sequence are of the same lithology as the rest of the



Figure 7. Tabular cross-bedding in the Minturn Formation. Note drab, gray-green color that is characteristic of the formation. Photograph was taken next to Wolf Creek on the Rainbow Trail.

Minturn Formation so that, for mapping convenience, they may be relegated to the Minturn Formation proper. This mapping procedure is consistent with Nolting's work (1970, Plate I) in the Orient--Cotton Creek area to the south.

Unit I consists of 250 to 300 feet of buff to gray, silty, largely recrystallized, crinoidal lime packestone (see Figure 8). The skeletal material includes foraminifera, crinoid stems, and echinoid spines, none of which can be used as index fossils. Most of the unit is a recemented breccia with angular fragments up to 3 feet across. Locally, some crude bedding and interbedded gray shale were found. Within the unit, the distribution of massive but discontinuous outcrops, combined with high concentrations of fossil material suggests a biohermal genesis. This hypothesis is further supported by similar occurrences, cited as bioherms by Peel (1971, p. 31-35), in the Cotopaxi inlier, and described by Berg (1967) in considerable detail, at approximately the same stratigraphic horizon.

The genesis of the breccia texture is uncertain. If it is accepted that the lime packestone was for the most part deposited in situ (i. e., not a monolithic conglomerate) as evidenced by the interbedded shales, lack of non-carbonate inclusions, and a fossil assemblage that differs markedly from that of older limestones in the area, then at least two possibilities exist. The brecciation may have occurred shortly after deposition by extreme turbulence during storms, when the accumulated carbonate material was

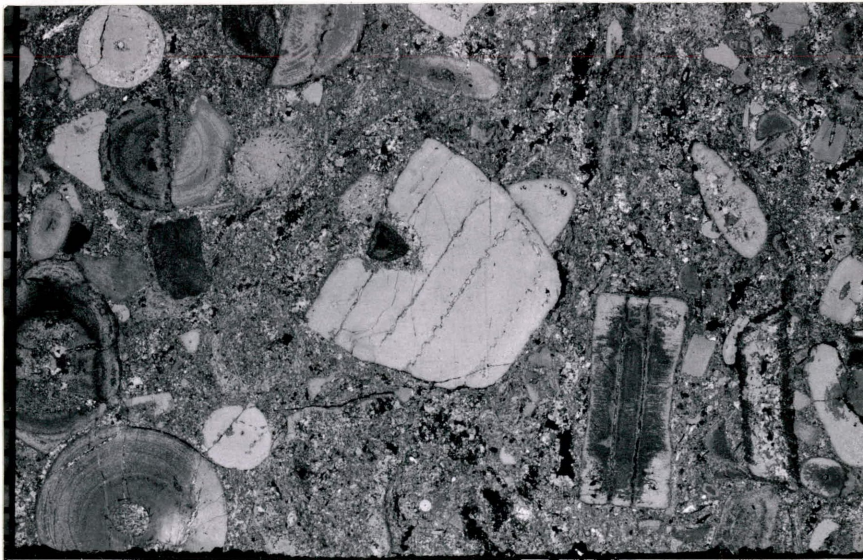


Figure 8. Photomicrograph of crinoidal lime packestone of Unit I. Scale in millimeters. Sample collected approximately 200 yards northwest of Big Cottonwood Creek.

only semi-lithified. Repeated organic buildup, semi-lithification, and storm disruption could account for the observed thickness of the breccia. A second plausible mechanism of breccia genesis is tectonic. The distribution of the unit, with an anomalously occurring sliver-shaped outcrop occurring along Pole Gulch (see Plate I), suggests that tectonic forces have been significant in the history of this rock. A post-depositional, pre-lithification, non-tectonic process is tentatively adopted as cause for the major amount of brecciation observed in Unit I. A repetitive storm disruption mechanism is envisioned which would agree with the hypothesized genesis of the unit (i. e., biohermal) and can better account for the great thickness of the unit than can a tectonic process.

Unit II is only about 40 feet thick near Big Cottonwood Creek but is an estimated 300 feet thick at a gypsum mine about $1\frac{1}{2}$ miles to the north. This thickening can be attributed to both tectonic folding (see Plate I) and lateral changes in depositional environment. The lithology of the unit is somewhat variable laterally but generally consists of medium-bedded, buff to gray lime wackestone that becomes more massive to the north. A gypsum component exists throughout the unit and varies in thickness from a few feet near Big Cottonwood Creek to over 200 feet at the

gypsum mine. Gypsum begins to occur in mineable quantities in Fox Canyon. No gypsum was reported by Nolting (1970) in equivalent units to the south. Farther to the northwest, near Hayden Pass Road, this unit is being mined extensively and the gypsum accumulation is probably quite thick. Brill (1952, p. 833) refers to this unit as the Swissvale Gypsum Member. Unit II is the product of a rapidly changing depositional environment, from an open shallow marine environment to one of restricted circulation, over a very short distance. The climate must have been warm and arid to account for the organic buildup of carbonates found in Unit I and to provide for high rates of evaporation needed to produce gypsum.

Fossils found within the limestone units and their equivalents, although often wide ranging, are generally Desmoinesian (Nolting, 1970, p. 33-99) or late Cherokeean (Peel, 1970) in age.

Sangre de Cristo Formation

The Sangre de Cristo Formation is exposed in a syncline near Big Cottonwood Creek and in the valleys formed by Fox Canyon Creek where the creek has cut through calcite-cemented pediment gravels (see Plate I). The formation has been subdivided into lower and upper members by Peel (1971, p. 46-60) based on Pierce's (1969) Units V and VI. Peel believes that the Crestone Conglomerate Member (Bolyard, 1959, p. 1923) of the Sangre de Cristo Formation is a coarser-grained facies of the upper member of the

Sangre de Cristo Formation. Although exposures are limited to a few stream cut areas, this author feels that only the lower member is present in the thesis area. Thicknesses reported by Peel (1971, p. 50) average about 3,800 feet for the lower member, and the total thickness of the Sangre de Cristo exposed in the area is 1,150 feet less than this. Also, the unconformity and marked increase in grain size which is said to exist at the contact between the members was not observed.

The lithologies of the lower member of the Sangre de Cristo Formation include red, maroon, and grayish-red, arkosic, pebble conglomerates, sandstones, siltstones, and shales. The conglomerates have an arkose sandstone matrix and consist of well-rounded, pebbles and occasional cobbles of Precambrian lithologies (mica-schist, gneiss, and granite). The sandstones are poorly sorted, arkosic, cross-stratified and range from fine to coarse grained. The siltstones and shales are often micaceous.

The lower contact of the Sangre de Cristo Formation is placed where the greenish feldspathic sandstones, siltstones and dark shales of the Minturn Formation give way to the red and maroon lithologies of the Sangre de Cristo Formation.

It is from the red color of this formation that the Sangre de Cristo Range received its name. Walker (1967) has explained the red color of Pennsylvanian and Permian clastic rocks in central Colorado by analogy with red beds currently being formed on Baja California. He has cited the wide

occurrence of Pennsylvanian and Permian evaporites to signify a regionally arid climate. Walker has demonstrated that the hematite which colors these rocks is a post-depositional alteration of unstable iron-bearing grains. These iron-bearing grains, eroded from Precambrian rocks exposed in the highlands, were able to be deposited before being altered because of the arid climate, high relief, and short distance of transport. He cites coalescing alluvial fans extending from the mountain areas and forming bajadas as the depositional environment for this process.

The contact between the Minturn and Sangre de Cristo formations is poorly exposed in the thesis area. On the northeast side of syncline K, situated near the junction of Big and Little Cottonwood creeks, the contact is sharp but concordant. Pierce (1969, p. 29) suggests the possibility of an unconformity between his Unit III (Minturn equivalent) and Unit IV (lower Sangre de Cristo equivalent), and Brill (1952, p. 811) cited the absence of post-Desmoinesian beds as evidence for an unconformity. Peel (1970, p. 38-40) shows evidence for an angular unconformity at the contact of these two formations. Observations of the contact made in the thesis area, in light of observations made by Pierce to the north and Peel to the south, suggest one of two possibilities: (1) the thesis area remained relatively low (compared to surrounding areas) and was not subjected to

erosion at the end of Pennsylvanian time and therefore no unconformity exists in the thesis area. (2) A regional angular unconformity exists, but since the degree of discordance varies from locality to locality as a function of the structure of the older unit, there is an essentially concordant relationship in the thesis area. The author prefers the latter explanation since Pierce and Peel had better exposures of the contact and the absence of post-Desmoinesian strata strongly suggests erosion.

Pollen found and identified by Scott (1967) in the lower part of the overlying Sangre de Cristo Formation suggest a Permian age for this unit. Since Missourian and Virgilian strata (Late Pennsylvanian) are probably missing from the record (Brill, 1952, p. 811; Peel, 1971, p. 46), it appears that the Minturn--Sangre de Cristo contact also represents the boundary between Pennsylvanian and Permian time.

Mesozoic Rocks

No sedimentary rocks of Mesozoic age are present in the Hayden Pass--Orient Mine area. Although the Front Range and Uncompahgre highlands were reduced to low relief, they persisted as positive elements from Triassic through Middle Jurassic time. It is probable that a considerable

thickness of the Morrison Formation was deposited over the area when the sea encroached upon the central Colorado highlands late in the Jurassic. During most of Cretaceous time, the sea repeatedly transgressed and regressed over Colorado and as much as 5,800 feet of Dakota, Benton, and Pierre lithologies may have been deposited over the Hayden Pass--Orient Mine area (Oriol and Craig, 1960). The early pulses of the Laramide orogeny, during Late Cretaceous, caused the sea to recede from the region (Haun and Weimer, 1960). The ensuing uplift resulted in erosion of all Mesozoic rocks from the thesis area.

Cenozoic Rocks

Tertiary Intrusive and Volcanic Rocks

One stock-like body and two dikes are exposed within the thesis area. Although no volcanic rocks were mapped, some evidence was found that suggests their presence.

Slide Rock Mountain Intrusive

The stock-like intrusion, which is located in the vicinity of Slide Rock Mountain, is semi-elliptical in outcrop pattern and includes about 2 square miles of exposed igneous rock (see Plate I). The rock generally consists of a white, fine grained, biotite-quartz monzonite (see Figure 9). Outcrops of this rock are characterized by large areas of white talus scree material from which Slide Rock Mountain derives its name. Although no extensive study of this

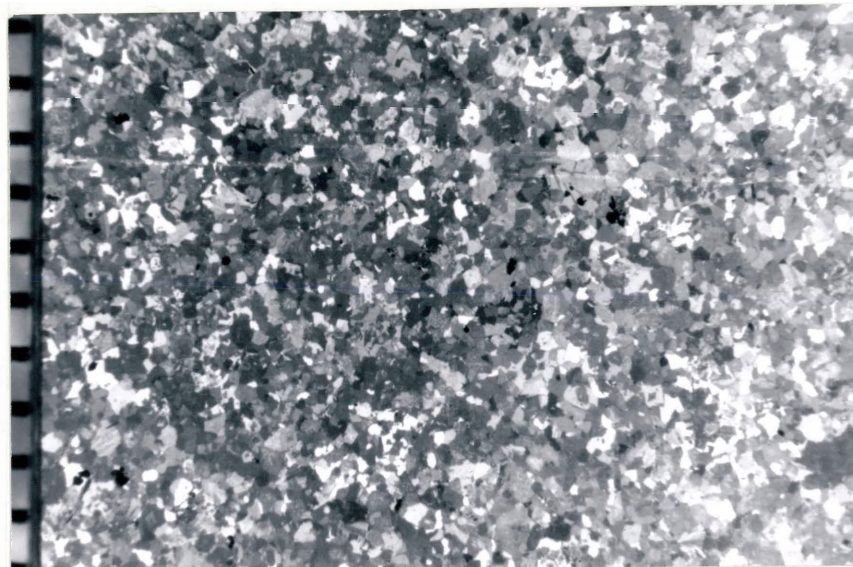


Figure 9. Photomicrograph of biotite-quartz monzonite of Slide Rock Mountain Intrusive. Scale in millimeters.

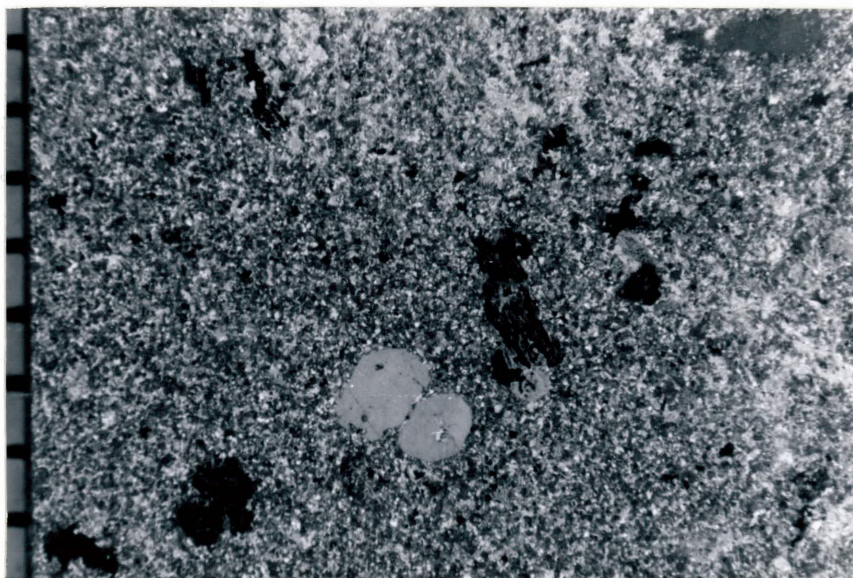


Figure 10. Photomicrograph of quartz-lattice porphyry of dike located on crest of the range. Scale in millimeters.

intrusion was undertaken, no significant lithologic changes were noted within the igneous mass, nor was any appreciable alteration or mineralization observed at its contact with the sediments. The fact that no contact metamorphism was observed is most probably an indication of the very poor exposure of the contact and the relatively small amount of field investigation rather than a lack of contact metamorphism. The intrusion is bounded on the southwest and cut in the northeast by inferred faults which probably were significant in the emplacement of this intrusion. A much smaller igneous body of similar lithology, which is believed to be an offshoot of the main intrusive mass and connected to it below the surface, was mapped in Pole Gulch (see Plate I). The main intrusion is probably a stock as suggested by the size and shape of the outcrop, as well as the observed high-angle, discordant contact relationships. The name Slide Rock Mountain Intrusive is informally given to this igneous body.

At least three lines of evidence indicate that the Slide Rock Mountain Intrusive is Tertiary (or latest Cretaceous) in age. First, the intrusive is on line with a series of Late Cretaceous-early Tertiary intrusives extending from Crestone Peak to the Park County line (Stose, 1935). The ages of two adjacent intrusions have been established. The Whitehorn Stock (northeast of Salida on the Park County line) has been radiometrically dated at 69 million years (G. R. Scott, 1971, oral communication) and the Rito Alto Stock (south of the thesis area) is estimated to be middle Eocene based on stratigraphic data (Burbank and Goddard, 1937, p. 975). If it is assumed that the series of stocks are related both

genetically and in time, then the Slide Rock Mountain Intrusive is probably of an intermediate age. Secondly, the Slide Rock Mountain Intrusive has been only slightly deformed by post-emplacement tectonics. This suggests that the intrusive was emplaced after (or during the waning stages of the Laramide orogeny. Lastly, a Tertiary (Eocene) erosion surface, established by Epis and Chapin (Epis, 1968, p. 56-59) and locally mapped by Nicolaysen (1971, p. 28-31), cuts the top of the intrusive. In order to be cut by this surface of erosion, the Slide Rock Mountain Intrusive must have been emplaced during or previous to Eocene time.

Igneous Dikes

Two igneous dikes crop out along the crest of the range. The southern-most one, which lies partly out of the map area, was not inspected nor mapped in its entirety. The other dike consists of a white, fine-grained, quartz-latitude porphyry (see Figure 10). The contact with the surrounding sedimentary rocks is discordant. Both dikes are in or near the Nipple Mountain syncline but have not themselves been folded. The close proximity of the dikes to the Rito Alto Stock, which occupies the crest of the range immediately to the southeast, suggests that their emplacement is related to that of the stock. Litsey (1954, p. 87) supports this relationship in citing the similarity in composition between the dikes and a rhyolite phase of the Rito Alto Stock.

A detailed report on the Rito Alto Stock has been written by Toulmin (1953). The stock is estimated to be middle Eocene in age based on debris found in the Cuchara Formation of that age in Huerfano Park (Burbank and Goddard, 1937, p. 975).

Volcanic Rocks

No volcanic rocks were mapped in the thesis area. However, on the south side of Hayden Pass Road near the bases of Trash and Italian gulches, there is considerable volcanic float. The float consists of pale-pink, hornblende-biotite latite. This may suggest that a lava flow, which has subsequently been eroded and covered by pediment gravels and alluvium, once filled the valley cut by Hayden Creek.

An excellent exposure of a crudely stratified, water-laid, volcanic conglomerate and an underlying biotite-trachyte flow occurs southeast of the thesis area. The conglomerate is approximately 60 feet thick along Little Cottonwood Creek and displays cut and fill structures and boulders up to 3 feet across. Crude stratification in this rock strikes N14E and dips 30E. About 30 feet of the underlying flow is exposed at this location. These volcanic rocks are no doubt the result of a major episode of vulcanism that occurred in the region during Oligocene time (Steven and Epis, 1968).

Quaternary Deposits

Glacial Deposits

Several geomorphic features attest to the alpine glacial activity that recently existed in the northern Sangre de Cristo Mountains. A well-developed cirque exists on the north side of Nipple Mountain, which presently retains snow late into the summer (see Figure 11). Small lateral moraines were observed in some valleys, but only the largest, which occur in Black Canyon, were mapped. Immediately south of the map area occur rock glaciers, which Nolting (1970, p. 55-61) has described in detail. He reports that the genesis of these interesting features is largely dependent on previous glacial activity.

Pediment Gravels

Pediment gravels were mapped on the east side of the range near the Arkansas River. The pediment surfaces represent at least two different episodes of extended bedrock erosion. The gravels on these surfaces are mapped as one unit. A well-defined topographic break occurs between pediment surfaces and the alluvium of the Arkansas River floodplain. The gravels generally consist of sub-angular to rounded, pebble to boulder size lithoclasts that often display a discoidal shape. The lithologies of the clasts include both sedimentary rocks of the Paleozoic section (about 30 percent) and crystalline rocks of the Precambrian



Figure 11. Cirque on north side of Nipple Mountain. Note occurrence of snow in late July when this photograph was taken.

basement (about 70 percent). Except along Hayden Pass Road, no volcanic clasts were noted. The gravels are loosely consolidated with a silt and mud matrix, and crude stratification indicates primary dips of 1 to 5 degrees northeast.

Special attention was paid to a calcite-cemented gravel occurring in the vicinity of lower Fox Canyon Creek. In order to better understand its genesis, this unit was mapped separately from the other pediment gravels. Near the lower reaches of Fox Canyon Creek, the well cemented gravel is about 10 feet thick, includes boulders up to 1 foot in diameter, and is more resistant than the underlying Sangre de Cristo Formation. The unit thins and becomes almost pure travertine in the vicinity of Fox Canyon. The farthest upstream occurrence is near a small spring in Fox Canyon where the unit is only about 2 feet thick. The areal distribution of this gravel cap suggests an original delta-shaped depositional pattern, emanating from Fox Canyon (see Figure 12).

As indicated on Plate I, this small spring is located within limestone Unit II. The evidence indicates that the small spring in Fox Canyon was at one time more active than it is today and was possibly warm or hot. Calcium carbonate, dissolved from surrounding limestone by the spring water, was precipitated in the gravels, cementing them into resistant cap rock. This interesting relationship

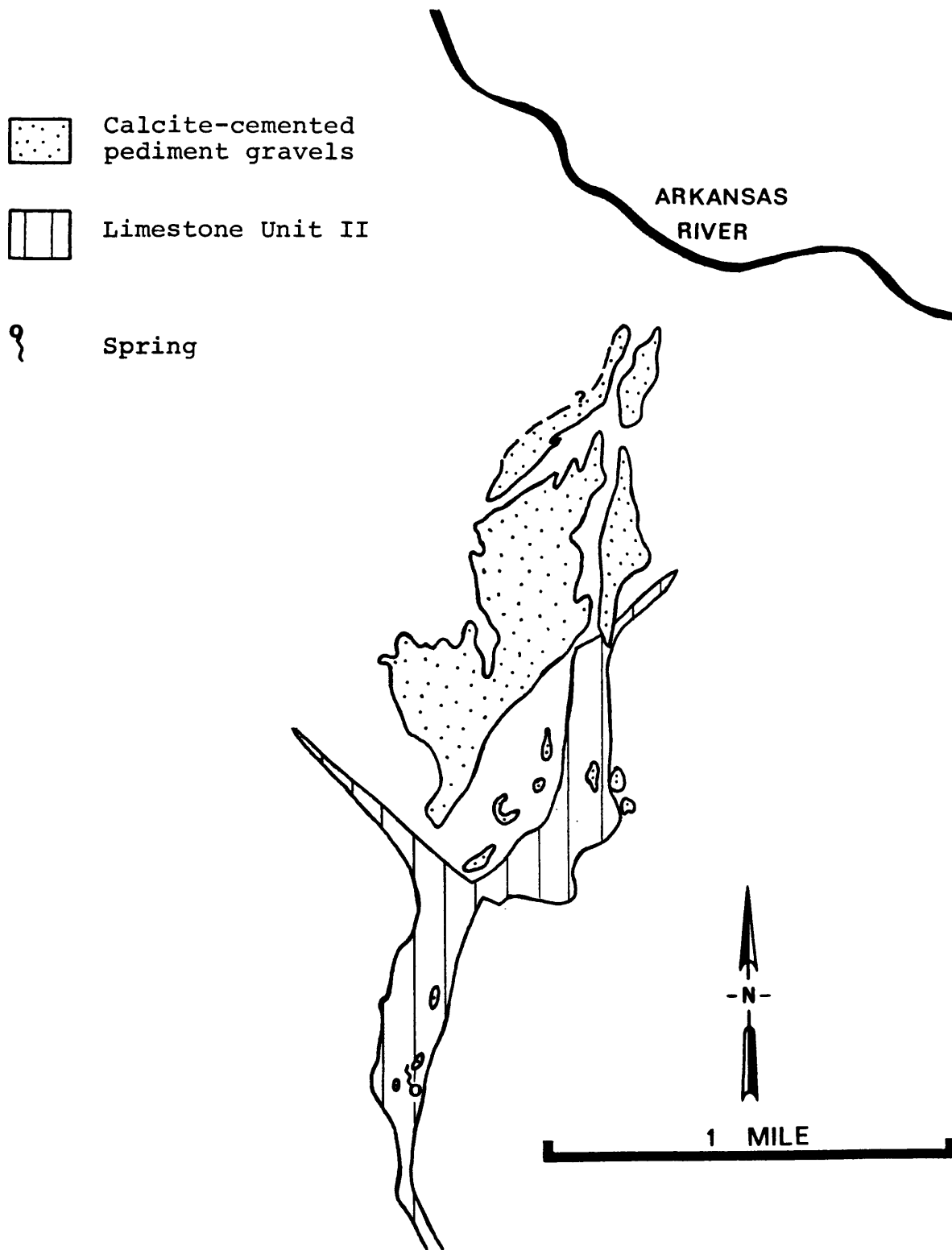


Figure 12. Map of distribution of calcite-cemented pediment gravels and limestone Unit II. Note location of spring in the limestone unit upslope from occurrence of calcite-cemented gravels.

was observed in similar situations by Peel (personal communication, 1971) in the area northwest of Hayden Pass Road.

San Luis Valley Alluvial Fans

The coalescing fans that exist west of the base of the mountains in the San Luis Valley represent recent geologic history during which older alluvial fans have been continually eroded, covered, and finally replaced by younger fans. This process has produced geomorphic and vegetation characteristics which facilitate subdividing the alluvial fans into correlatable units of similar age. The classification and correlation scheme as developed by Knepper (1972) has been adopted for this thesis. The oldest fans in the area are highly dissected, sparsely vegetated, steeply sloped, and of intermediate size. Somewhat younger fans are labeled Qaf III and are of large extent. These fans are less dissected than Qaf IV fans, are steeply sloped, and are sparsely vegetated. The surface of Qaf IV fans is generally above the surface of Qaf III. The alluvial fan designated Qaf II is quite young, very large, gently sloped and is not significantly dissected. The boundary between this fan and older surrounding Qaf III fan material is locally vague. The surface of Qaf III fans is generally higher than that of Qaf II fans. The youngest fans, designated Qaf I, occur in the immediate vicinity of the base of mountains as small, steeply sloped cones. They represent the initial stages of alluvial fan development.

The degree of precision with which the fan units may be correlated is largely dependent on proximity. Fan units

within the thesis area can be correlated with some confidence, but correlation of fan units in widely separated areas of the San Luis Valley may not be valid.

Scott (1970a, p. C17) cites the age of the alluvial fans as being Bull Lake and Pinedale. Episodes of fan building and erosion, which produce a group of alluvial fans with similar ages, are probably related to climatic changes occurring during the Pliocene. Scott (1953, p. 48-49) outlines a geomorphic cycle in which erosional and depositional processes, as recorded by land forms, are correlated with climatic fluctuations. A cycle is initiated as the climate becomes colder and wetter, resulting in glaciation in the mountains and increased stream load and rates of discharge. Downcutting and erosion of preexisting alluvial fans occur during this phase of the geomorphic cycle. As the climate becomes warmer and drier, load begins to overbalance discharge and sideward stream cutting of the preexisting alluvial fans ensues. Because this process did not continue to completion, remnants of fan units Qaf IV and Qaf III exist in the thesis area. When the climate becomes still warmer and more arid, the balance of load to discharge becomes still greater and deposition of a new group of alluvial fans begins. As the climate becomes cooler and wetter, the cycle begins anew. The youngest alluvial fans, designated Qaf I, have apparently developed since the last period of glaciation and should be considered to be Holocene in age.

STRUCTURAL GEOLOGY

Figure 13 shows major structural features of south-central Colorado. The Pleasant Valley fault, and other related faults to the north (Mosquito-Weston fault, London fault, and Elkhorn thrust), were initiated during Permo-Pennsylvanian deformation and were probably instrumental in the uplift of the Front Range--Wet Mountain highland (Pierce, 1969; Nolting, 1970, p. 80-82; De Voto and others, 1971; De Voto, 1972; Peel, 1971, p. 61-63]. During the Laramide orogeny, compressive forces developed a series of approximately north-south arches and basins. A very large anticlinorium was formed west of South Park that includes the present-day Sawatch, Mosquito, and northern Sangre de Cristo mountain ranges. Gabelman (1952) refers to this anticlinorium as the Sawatch arch.

The modern Sangre de Cristo Mountains and the adjoining San Luis Valley are of later origin than the Sawatch arch and related structures of the Laramide orogeny. These large structural features are the result of Basin and Range style deformation, characterized by the Sangre de Cristo fault. The exact nature of the San Luis Valley is not well understood, but Gaca and Karig (1966) have suggested that a

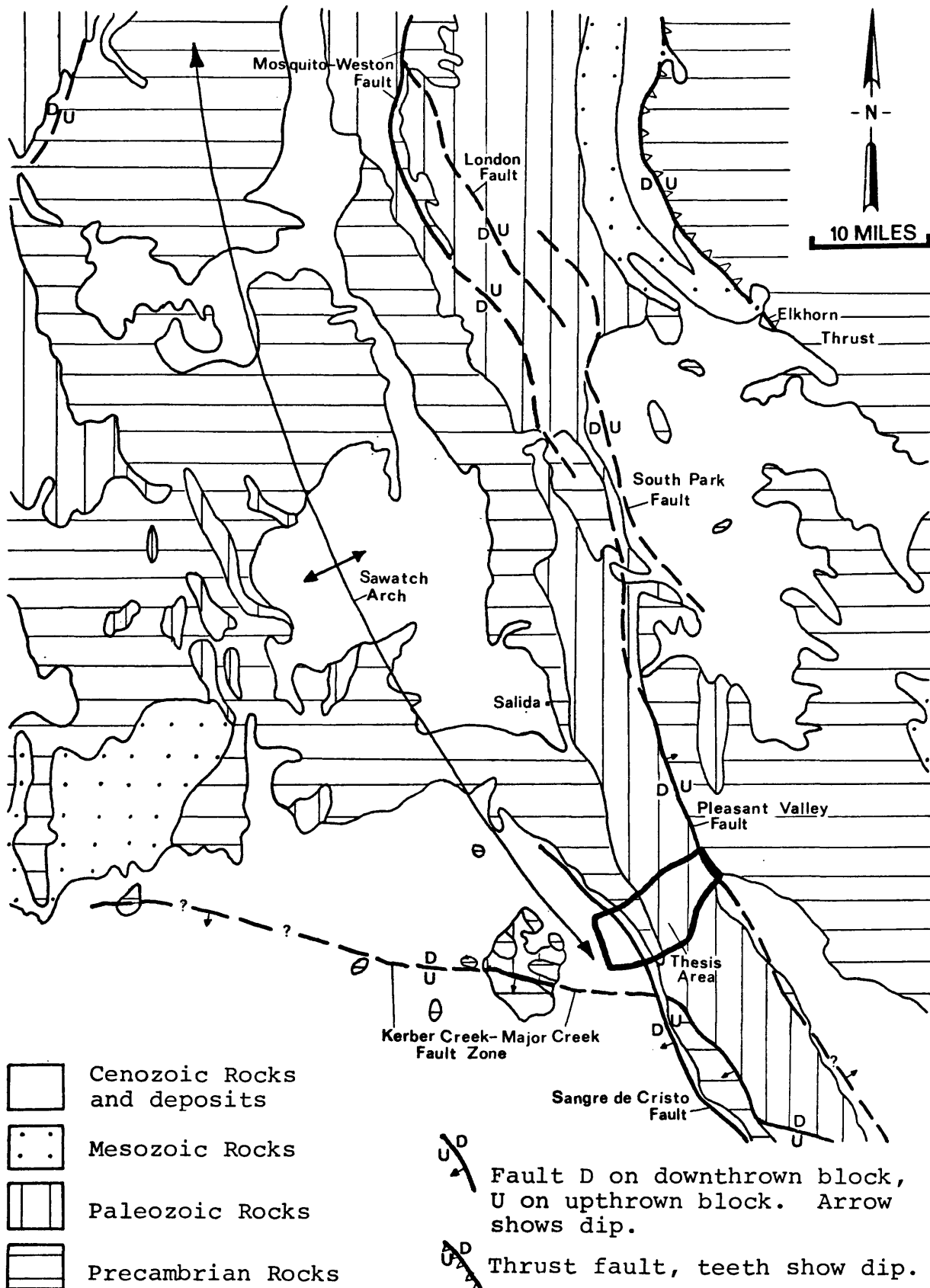


Figure 13. Regional tectonic features of south-central Colorado (modified from "Configuration of Precambrian," Mtn. Geol., Oct. 1969; and Stose, 1935).

deep graben exists beneath the valley floor based on gravity measurements.

Folding

At least 17 folds exist in the Hayden Pass--Orient Mine area of which eight may be considered as major structural elements (Plate I). Most of the fold axes trend north-south or northwest-southeast, which generally coincides with the trend of the mountain range. Litsey (1954) reports that the tightest folding in the northern Sangre de Cristo Mountains occurs within the thesis area.

Folds on the West Slope

Pre-Pennsylvanian and Lower Pennsylvanian units have been tightly folded in the vicinity of Steel, Lime, and Black canyons (see Figure 14). The Steel Canyon anticline extends from Black Canyon north to slightly beyond South Piney Creek, and is well expressed topographically by the resistant Leadville Limestone in Steel Canyon. This asymmetrical fold has a steeply dipping west limb which in some places approaches vertical, and an east limb which dips between 40 and 60 degrees. The Chaffee Formation is exposed along the fold axis in Black, Lime, and Steel canyons and a small exposure of Fremont Dolomite was mapped on the south side of Steel Canyon.

The Steel Canyon syncline parallels the Steel Canyon anticline to the west. This syncline is overturned to the

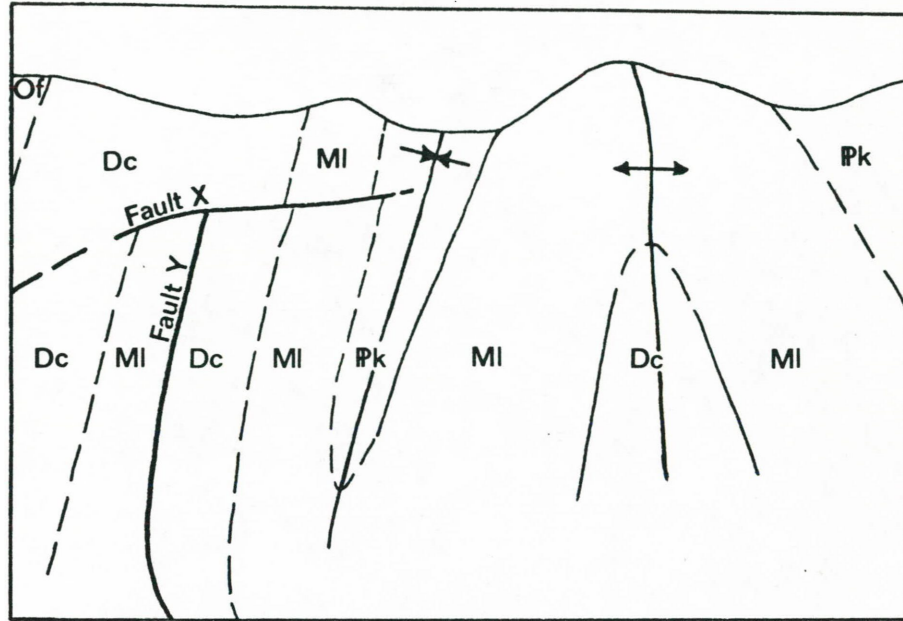


Figure 14. Photograph of Steel Canyon anticline and overturned Steel Canyon syncline. North side of Lime Canyon. Of = Fremont Dolomite; Dc = Chaffee Formation; MI = Leadville Limestone; Pk = Kerber Formation.

east in Lime Canyon where it is best exposed (see Figure 14). The fold is faulted in four different areas and terminates against a fault (fault Y) in Lime Canyon.

Two southeast plunging folds (folds A and B, Plate I, Section A-A'), an anticline and syncline, occur near Hayden Pass and are broken near their axis by reverse faults. The small anticline, which is centered right on Hayden Pass, is cut by the Galena Peak Fault. The Galena Peak Fault, as mapped by Litsey (1954), dies out as it enters the thesis area. The syncline, which lies to the southwest of the anticline, is cut near its axis (especially to the northwest as mapped by Litsey, 1954) by the Silver Creek Fault.

Two small folds (folds C and D, Plate I) are situated on the crest of the range northwest of Nipple Mountain. These folds appear to die out a short distance both north and south of the crest. Folds C and D are considered to be small, minor folds within the Nipple Mountain syncline, a major fold to the east (see Section D-D', Plate I).

Folds on the East Slope

The Nipple Mountain syncline is a major fold. Nolting (1970) has mapped this structure to the south as it passes to the west side of the range. This syncline is very wide and open in the southern part of the area

(see Section C-C') but is complicated by smaller folds C and D near Nipple Mountain. A major anticline (E, Plate I) parallels the Nipple Mountain syncline to the east.

The Wolf Creek syncline and Wolf Creek anticline are well defined on Wolf Creek. Both folds are expressed by the topography in the north but apparently die out south of Millball Gulch. The Wolf Creek anticline appears to terminate against fault P just north of Wolf Creek. Two minor folds (F and G, Plate I) were mapped east of the Wolf Creek folds which apparently are terminated to the north by an inferred fault. The southern extent of these folds is not known.

Between Middle and South Prong of Hayden Creek, are three generally east plunging folds (H, I, and J, Plate I). These minor folds are oriented normal to the Nipple Mountain syncline and may be separated from it by a fault of right-lateral separation. Field and remote sensor data, however, did not support the placement of a fault in this area.

In the northeast section of the thesis area is a southeast plunging syncline with Sangre de Cristo Formation preserved in the center (K, Plate I, Section B-B'). Syncline K appears to be the northern end of the large Spread Eagle syncline that is mapped to the south by Nolting (1970). The genesis of this syncline, at least in part, is by drag along the reverse fault S that bounds the fold on the

northeast (see Section B-B'). On the north side of fault S is a small easterly plunging anticline (L, Plate I, Section B-B') that also may have been formed by drag along the fault.

Fold M is a small northeast-plunging syncline, largely covered by pediment gravels, that is defined by attitudes taken in the Sangre de Cristo Formation where it is exposed by Fox Canyon Creek. This structure is complicated by other small folds and faults too small to map.

Faulting

In general, fault traces within the Hayden Pass--Orient Mine area are poorly exposed because of thick vegetative cover, extensive soil development, and talus deposits. Most faults are inferred based on stratigraphic repetition or omission, disrupted bedding, breccia zones, and remote sensor data as discussed in the text. Displacements indicated on the cross sections of Plate I are rough estimates only.

In this thesis, the faults of the area have been grouped, where possible, based on geometry, relative movement, and, to a lesser extent, on location. Except for faults classified as of "unknown geometry", the groupings are presented in a general chronological order from oldest events to those occurring very recently.

Hypothetical and Inferred Faults of Unknown Geometry

Several faults exist in the thesis area which have

been mapped based on sketchy field evidence and/or remote sensor data. The geometry and relative movement along these faults is largely unknown so they are discussed under a separate heading.

Three subparallel, inferred faults (N, O, and P, Plate I) have been mapped in the vicinity of Table, Slide Rock, and Rattlesnake mountains that trend northwest. Fault N can be seen in outcrop northwest of Hayden Pass Road but relative movement could not be determined. Bedding attitudes and the linear boundary of the Slide Rock Mountain Intrusive suggest the presence of this fault to the southeast. Placement of faults O and P is based primarily on lineaments found on small scale photography. On Hayden Pass Road, outcrops show bedding to be disrupted by small faults and gouge zones on both sides of the fault O (see Figure 15). The fault itself occupies a small drainage and is not exposed. Bedding attitudes next to the fault O indicate upward movement on the northeast side of the fault. The surface traces of faults O and P indicate sub-vertical, possibly northeast dipping, fault planes.

Fault Q is an inferred fault mapped subparallel to and southeast of Pole Gulch that extends into the vicinity of Fox



Figure 15. Fault, gouge, and disrupted bedding zone on northeast side of inferred fault O on Hayden Pass Road.

Canyon. Fault Q is substantiated by: (1) an anomalous sliver of Unit I in Pole Gulch; (2) the abrupt end to Unit I in Pole Gulch; (3) divergent bedding attitudes just northwest of Fox Canyon; and (4) truncation of Unit II northeast of Fox Canyon Creek. The fault trace suggests a sub-vertical fault plane but relative movement could not be ascertained.

Fault R, which is of probable major magnitude, is concealed in the thesis area by Quaternary deposits. The location of fault R is based on low-angle-illumination photography of a raised topographic relief map (Pueblo, NJ13-5, series V502P) and mapping done by Peel (1971) in the vicinity of Middle Prong. Peel's geologic map suggests a small amount of right separation and unknown vertical displacement. The fault appears to die out 2 miles west of Hayden Creek Campground, but is well expressed topographically to the east.

Reverse Faults Near the Arkansas Valley

A major reverse fault occurs in the northeast part of the map area. The Pleasant Valley fault enters the area from the northwest, buried by alluvium of the Arkansas River. This major fault continues, after possible right lateral offset, along Falls Gulch east of the thesis area. This fault has been described

(Gabelman, 1952, p. 1596) as a high-angle, east-dipping fault that has faulted Precambrian Pikes Peak Granite over Paleozoic sediments. This is the case north of the thesis area. However, east of Big Cottonwood Creek, Precambrian rocks have apparently been faulted onto Precambrian rocks along this same fault. Reconnaissance work in the Falls Gulch area has shown different sets of joints and a change in crystal size from one side of the gulch to the other. The fault trace itself is covered.

Fault S, which has similar reverse motion, has been inferred from the mouth of Pole Gulch southeast to Little Cottonwood Creek. This fault is based on: (1) gouge zones and distortion of beds within the Sangre de Cristo Formation on the south side of Little Cottonwood Creek, (2) offset of limestone Unit II, (3) distribution of poorly bedded or unbedded gypsum of Unit II along the southwest side of the fault, and (4) the abrupt and linear start of higher topography near the mouth of Pole Gulch. This topographic break is interpreted to be an obsequent fault-line scarp since lower topography exists on the upthrown side of the fault line.

A problem exists concerning the relationships observed near the mouth of Little Cottonwood Creek. Here, fault S bifurcates, leaving a small area of Minturn Formation on the north side of the creek between fault S and fault T. Two outcrops

of brecciated rock exist on either side of Big Cottonwood Creek, both of which are believed to be on the trace of fault T. Evidence for faulting was lacking to the northwest of these outcrops, where a line defined by the two breccia zones would trend. It is inferred that fault T turns sharply to the north and is located beneath the alluvium of Big Cottonwood Creek between Precambrian crystalline rocks and Paleozoic sedimentary rocks. The sense of movement on this inferred fault is probably similar to that of the Pleasant Valley fault.

Longitudinal Faults Related to Folding on the West Slope

Several faults exist in the pre-Pennsylvanian rocks which generally parallel and lie close to fold axes. Because of their position relative to the folds, and the fact that most of them indicate reverse motion, it is probable that they are related to the last episodes of folding in the area.

The Silver Creek and Galena Peak faults are high angle reverse faults which dip east. Litsey (1958) reports that the Galena Peak fault appears to be a hinge fault beginning near Hayden Pass and increasing in displacement toward the northwest. The surface trace of this fault was not detected or mapped within the thesis area. The Silver Creek fault (Section A-A') extends out

of the mapped area to the north and into Precambrian rocks near North Piney Creek to the south. In addition to vertical movement, a component of right lateral displacement is suggested by a small drag fold developed in the Harding Sandstone on the west side of the fault. Displacement along this fault appears to be greater toward the south.

Two small subvertical faults (U and V, Plate I) are located near the axis of the Steel Canyon anticline as shown in Section D-D'. The dip of the fault planes is not known, but the block between the faults has been moved up relative to the adjoining blocks. The location of an outcrop of Leadville Limestone, faulted into the center of the Steel Canyon syncline, may indicate a component of left-lateral displacement.

A strike fault (W, Plate I) has been inferred southwest of faults U and V that involves Leadville Limestone, Chaffee Formation, and Fremont Dolomite. The basis for mapping fault W is a change in dip from 75 degrees in the Harding Sandstone to 10 degrees in the Fremont Dolomite as observed in Steel Canyon, and an anomalous thickness of Chaffee Formation north of Steel Canyon. The sense of displacement on this fault is not known.

Faults X and Y are closely related faults that extend from Black Canyon north to just beyond Lime Canyon. These faults probably dip steeply to the west. In the vicinity of Lime Canyon,

fault X certainly dips west, possibly by as much as 45 degrees. The exact locations of these faults can be determined in only a few places where rock units are displaced and must be inferred where only anomalous stratigraphic thickness indicates their presence.

Transverse Faults on the West Slope

Several small faults, which are normal to structural trend and bedding strike, are on the west flank of the mountains. Horizontal separation is generally quite small.

Two transverse faults (Z and AA, Plate I) of considerable magnitude occur in the vicinity of Steel Canyon. They define an angular block of Precambrian rock which has been faulted up and into the Paleozoic sediments. Displacement along fault Z has offset the Steel Canyon syncline and anticline and has drag folded the Leadville Limestone indicating right-lateral separation increasing toward the south. A component of vertical displacement may exist on the southern portion of this fault to account for the large amount of displacement necessary to place Precambrian rocks against Leadville Limestone.

Normal Faults in the San Luis Valley

The most recent tectonic activity in the area has occurred along normal faults located at the boundary between the Sangre de Cristo Mountains and the San Luis Valley, and in the San Luis Valley proper.

The Sangre de Cristo fault is covered throughout most of its length by alluvial fan material. The fault trace is well expressed by vegetation in the vicinity of

Oak Springs, northwest of Hayden Pass Road. Also, alluvial fan material has been vertically offset about 15 feet at the mouth of Steel Canyon. Further evidence for a major fault in this area includes: (1) eroded, triangular-faceted spurs along the mountain front (see Figure 2); (2) the linear, well-defined mountain-valley boundary, (3) hot springs at Valley View Hot Springs (1 mile southeast of the Orient Mine); and (4) several small fault scarps in the San Luis Valley, sub-parallel to and indicating similar movement as the Sangre de Cristo fault. The vertical displacement on this fault may be much greater than estimated in the cross sections of Plate I (Litsey, 1958, p. 1168).

Several small fault "scarplets" (use of Blackwelder, 1928, p. 303-304), most of which face southwest, were mapped in the San Luis Valley. These scarplets, which are formed in alluvial fan material, are believed to be the surface expression of recent normal faulting associated with the Sangre de Cristo fault. Evidences to support these features as being fault generated includes the following: (1) they form a hydrologic barrier in the vicinity of Piney Creek; (2) they crosscut the local drainage, so could not be a drainage feature of cut and fill; (3) they branch, are

locally discontinuous, and are independent of elevation, unlike terrace features that might be related to San Luis Creek. Also supporting the fault genesis of these scarplets, and relating them to the Sangre de Cristo fault, is apparent bifurcation of the Sangre de Cristo fault near Valley View Hot Springs, 1 mile southeast of the Orient Mine (Scott, 1970a, p. C16-17). The southwest branch of the Sangre de Cristo fault, discussed by Scott, trends into and has similar topographic expression as those mapped in the thesis area.

Total relief on the fault scarplets occurring within the thesis area varies from almost nothing to about 8 feet. Scott reports that the scarp near Valley View Hot Springs is 25 feet high. The amount of displacement along these faults is unknown and probably cannot be based on the amount of displacement suggested by the height of the fault scarps. The geometry of the scarplets suggests that most of the faults are steeply dipping to the southwest. Exceptions are three fault segments, (BB, Plate I) mapped near San Luis Creek (see Section D-D'), which display northeast sloping scarplets suggesting normal faulting with movement opposite to the faults immediately to the northeast. More discussion of these faults can be found in the remote sensing section of this thesis.

Structural History

The Rocky Mountain region ("Rocky Mountain region" used here as defined by Grose (1972, in press), in general, has been subjected to epeirogenic movements throughout most of the Paleozoic and Mesozoic. Limited areas of the region were affected by Permo-Pennsylvanian deformation. Near the end of the Cretaceous, the region was subjected to the beginnings of the Laramide orogeny. The regional uplift and compressional forces of the Laramide orogeny developed most of the structural elements which are found in the Rocky Mountain region today. For purposes of this thesis, the term Laramide orogeny refers to a "deformational episode no older than Late Cretaceous and no younger than Eocene" (Dennis, 1967). Since Eocene time, the Rocky Mountain region as a whole has experienced epeirogenic uplift.

The thesis area and parts of the surrounding region are unique within the framework of the Rocky Mountain region. This area has been structurally affected by three major episodes of tectonic activity. Similar to the rest of the Rocky Mountain region, epeirogenic oscillations near sea level prevailed during the early and middle Paleozoic.

Ancestral Rocky Mountain Orogeny

Starting in Late Mississippian time, the area was uplifted as the tectonic stresses which produced the Ancestral Rockies began. This episode of deformation was manifested dominantly by subvertical faulting which bounded the Uncompahgre highland, the Front Range--Wet Mountain highland, and the intervening Central Colorado trough (Figure 5). The Pleasant Valley fault, and other reverse motion faults mapped near the Arkansas River, were initiated during this time (De Voto, 1971; Peel, 1971; Pierce, 1967; and others).

Laramide Orogeny

Sometime during Late Permian, epeirogenic tectonic movements again prevailed with alternating periods of deposition and erosion occurring until the end of the Cretaceous (Oriel and Craig, 1960). The beginnings of the Laramide orogeny produced general uplift and resulting erosion. The rocks of the Rocky Mountain region were subjected to horizontal compressional stresses. That most of the folds and faults of the mountainous part of the thesis area are of Laramide age can be established by the process of elimination. Since much of the deformation has occurred to Pennsylvanian and Permian rocks (i. e., the Kerber, Sharpsdale, Minturn, and Sangre de Cristo formations), the episode of deformation must post-date the Ancestral Rocky Mountain orogeny. "Post-Laramide

tectonics" (discussed on p. 63) have been established to be extensional in nature (Chapin, 1971; Grose, 1972, in press). The folding and reverse faults of the mountainous parts of the thesis area could not be initiated by the tensional stresses related to this episode of deformation. This leaves the Laramide orogeny to account for the structural features of the mountainous part of the area. The majority of the folds mapped in the thesis area have a north to northwest orientation. This suggests that the Laramide stress field was directed east-northeast--west-southwest. Many of the faults described under the heading "Longitudinal Faults Related to Folding on the West Slope" are no doubt related to the last stages of folding where compressional stress has been translated into reverse sense displacement, rather than folding. The fact that the fault traces are generally near a fold axis and parallel to the axis, substantiates this theory. One of the longitudinal faults shown in Section D-D' (fault V) appears to be a high-angle normal fault and does not fit in with the idea of a compressional genesis. It may be that original reverse displacement on this fault was later negated by a larger component of normal movement associated with reactivation by taphrogenic stresses developed during a later tectonic event. The idea of subsequent normal movement on faults, originally developed as reverse faults, was suggested by Nolting (1970, p. 94) and Nicolaysen (personal communication, 1970) to explain structures in areas immediately south and north of the thesis area.

The folds that exist between Middle and South Prong display an anomalous orientation in relation to neighboring folds to the east but are sub-parallel to adjacent folds to the south. As mentioned previously, their normal orientation to the folds to the east may be due to a possible fault of right-lateral separation, east of South Prong, which was not mapable based on field or remote sensor data.

Faults N, O, and P are probably late Laramide features that may have been initiated prior to or during emplacement of the Slide Rock Mountain Intrusive. Post-emplacement activity on these faults is indicated by faulting of the intrusive. Although the sense of movement on these faults is uncertain, they may have been initiated as reverse faults during Laramide compression, followed by normal movement along these zones of weakness during relaxation of the compressional stress or during the following episode of taphrogenic tectonics.

After cessation of the Laramide orogeny, near the end of Eocene time, a short period of relative tectonic quiescence prevailed during which early Oligocene volcanic activity took place throughout the region (Epis, 1968).

Post-Laramide Tectonics--Taphrogeny

By Miocene time, a third major tectonic episode had begun. This episode is characterized by taphrogenic tectonics, similar to those which developed the Basin and

Range Province. The Rio Grande Rift Zone (Chapin, 1971), which extends from New Mexico up into south-central Colorado, is an extension of the Basin and Range Province into the Rocky Mountain region (Grose, 1972, in press). The San Luis Valley and the Sangre de Cristo Mountains are two fault blocks separated by a normal fault in classical "Basin and Range" style. This normal fault, which is the Sangre de Cristo fault, cuts Laramide structures south of the thesis area and Pleistocene alluvial fans of the San Luis Valley. The Hayden Pass--Orient Mine area is currently under the influence of this episode of extensional tectonics.

GEOLOGIC HISTORY

The Precambrian history of the area has not been studied. Lower and middle Paleozoic carbonates and sandstones were deposited on an eroded surface of Precambrian rocks. During this time, the area was near the southern edge of an east-west trough which was bounded by the low, positive areas of the Siouxi and Sierra Grande landmasses (Litsey, 1958, p. 1148). Stable shelf conditions provided for blanket-type deposits. Minor uplifts and associated erosion resulted in complete removal of the Sawatch Sandstone and disconformities between the formations. Uplift began during Late Mississippian time, marking the beginning of intense tectonic activity that resulted in widespread subaerial erosion of the Leadville Limestone (DeVoto, 1965, p. 22).

Tectonic activity, dominantly vertical faulting, continued into Pennsylvanian time, producing the mountainous Uncompahgre and Front Range highlands and the intervening Central Colorado trough (see Figure 5). This rapidly sinking trough received sediments throughout the Pennsylvanian and Early Permian from the two adjacent landmasses.

The Kerber Formation represents the earliest preserved deposits that accumulated in the Central Colorado trough. During this time of deposition, a combination of swamp, littoral, and near shore environments existed in the local area. This is suggested by thin coal seams (Burbank, 1933; Brill, 1952, p. 832; Pierce, 1969), quartz sandstones, and carbonaceous shales characteristic of the Kerber. The quartz was probably derived from erosion of lower and middle Paleozoic rocks exposed in the bordering highlands. Kerber lithologies interfinger with marine shales of the Belden Formation to the north (DeVoto, 1961), suggesting that the Central Colorado trough deepened to the north.

During Atokan time, a period of rapid uplift of the highlands is suggested by the thick wedge of coarse red clastics of the Sharpsdale Formation. Graded bedding, found throughout much of the formation, may be related to the rapid influx of sediments causing unstable slopes to develop on unconsolidated deposits with resulting small turbidity flows. Fluvial channels within the unit, as supported by cut-and-fill structures and lenticular shaped sand bodies, indicate a fluvial plain environment for parts of the unit.

Continued rapid uplift of the Uncompahgre and Front Range highlands, and associated subsidence of the depositional basin, enabled great thicknesses of feldspathic

sediments to be deposited. The 6,000 feet or more of Minturn Formation represents several depositional environments ranging from marine through continental. Cross-bedded sandstones, like those shown in Figure 7, were probably deposited on a fluvial plain. The limestone units near the top of the Minturn Formation are dominantly of marine (biohermal) origin, and the included gypsum deposits indicate a period of local basin restriction coupled with high evaporation rates. The limestone units indicate that uplift of the highlands during this time may have slowed or temporarily stopped, resulting in a decrease of detrital influx. After deposition of the limestone units, the entire area was uplifted, eroded, and slightly deformed as indicated by the postulated angular unconformity between the Minturn and Sangre de Cristo formations.

Renewed uplift of the highland areas during Early Permian time provided for accumulation of the thick Sangre de Cristo Formation. Most of the lower member of this formation was probably deposited on an alluvial plain by fluvial processes, but coalescing alluvial fans may also have been an important component as suggested by Walker (1967, p. 357).

Although not present in the thesis area, an angular unconformity is described by Peel (1971), Nolting (1970), and Pierce (1967), between the lower and upper members of the Sangre de Cristo Formation, which suggests that the area was uplifted, deformed, and eroded for a period of Permian time. Final uplift of the highland areas produced the Crestone Conglomerate which occurred as alluvial fans bordering the mountainous terrain. The finer grained equivalent of the Crestone Conglomerate, named the upper member of the Sangre de Cristo Formation by Peel, is probably a fluvial deposit (Peel, 1971, p. 69).

The reverse faulting inferred near the Arkansas River Valley was initiated during Pennsylvanian time as growth faulting indicated by a great change in thickness occurring in the Minturn Formation in this area. Peel (1970, p. 62-63) suggests that extension of this fault system to the southeast would closely align it with a fault zone which bordered the ancient Wet Mountain highland. The Pleasant Valley fault, and related structures which line up with it to the north (Mosquito-Weston fault and Elkhorn thrust), are probably part of this Permo-Pennsylvanian fault system which displays evidence of movement as late as Paleocene (DeVoto, 1961, p. 207; Litsey, 1958, p. 1171).

Although no Mesozoic rocks occur in the northern Sangre de Cristo Mountains, some generalities may be stated based on Mesozoic rocks which occur in other parts of

Colorado. Late Permian, Triassic, and Early Jurassic time was a period of general regional uplift and erosion (DeVoto, 1971, p. 72). During the Middle and Late Jurassic, the area of deposition encroached upon central Colorado and a considerable thickness of the nonmarine Morrison Formation was deposited (Oriel and Craig, 1960). The Cretaceous was marked by alternating transgressions and regressions of the sea over Colorado. The environments of deposition included marine, transitional, and continental (Haun and Weimer, 1960). Near the end of the Cretaceous, uplift caused the sea to retreat and thousands of feet of Jurassic and Cretaceous rocks were eroded from the area (Haun and Weimer, 1960, p. 64).

Starting in Late Cretaceous, the area was uplifted and deformed by the Laramide orogeny. Most of the folds and faults which occur in the mountainous part of the thesis area were developed during this episode of tectonism. Because Cretaceous and Tertiary sedimentary rocks are not present in the thesis area, the literature concerning these rocks in adjacent areas has been consulted in order to reconstruct the Tertiary geologic history.

Burbank and Goddard (1937) have interpreted early Tertiary structural events occurring in the Sangre de Cristo Mountains based on the Eocene Poison Canyon, Cuchara, and Huerfano formations which occur in Huerfano Park. Uplift and erosion of the deformed Paleozoic landmass

took place in the Paleocene as indicated by an unconformity between the Upper Cretaceous Vermejo Formation and the overlying Poison Canyon Formation. This uplift is probably related to the early stages of the Laramide orogeny. The coarse texture and the granitic rock fragments contained in the Poison Canyon Formation attest to the nearness of the uplifted areas. Burbank and Goddard interpret a climax of intense deformation by overthrusting during early Eocene, at a time after deposition of the Poison Canyon Formation but before deposition of the overlying Cuchara Formation. This episode of deformation continued into middle Eocene. Evidence cited for this tectonic activity is an angular unconformity between the Poison Canyon and Cuchara formations and a lesser unconformity between the Cuchara and Huerfano formations. The lithology of the Huerfano Formation suggests that the uplifted areas were reduced to minor topographic elements before the beginning of differential uplift of nearby Precambrian massifs. Burbank and Goddard suggest that it is this differential uplift, beginning in middle Eocene, that accounts for the present elevation of the mountains around Huerfano Park.

Intrusion of igneous rocks in the northern Sangre de Cristo Mountains took place during or after the last stages of the Laramide orogeny. The Rito Alto stock was emplaced during early or middle Eocene (Burbank and Goddard,

1937). Although the dikes on the crest of the range do not appear to have been affected by the stresses that have deformed the sedimentary rocks, the Slide Rock Mountain Intrusive has been faulted in three areas.

Uplift of the Sangre de Cristo Mountains and subsidence of the San Luis Valley had begun by the Miocene after extrusion of Oligocene ash flows which occur throughout the region (Epis, 1968; Scott, 1970b, oral communication). The earliest deposit in the northern San Luis Valley is the Miocene and Pliocene Santa Fe Formation. Deposition of this unit indicates that the San Luis Valley, as a negative feature, had been established by this time. Movement along the Sangre de Cristo Fault has proceeded from Miocene through Holocene as evidenced by the preservation of fault scarps in unconsolidated alluvial fan material. The area is currently under the influence of this latest taphrogenic episode of Basin and Range type tectonics.

During the Pleistocene, alpine glaciers eroded the upper parts of the Sangre de Cristo Range and morainal deposits accumulated in the larger valleys. Near the Arkansas River, gravels covered pediment surfaces. These pediment surfaces may have counterparts in the San Luis Valley, but if they exist, they are covered by thick alluvial fan deposits. The alluvial fans that make up the surface of the San Luis Valley were probably

deposited from late Pleistocene through Holocene. Alluvial fans mapped as Qaf I are currently being developed at the mouths of some valleys.

APPLICATIONS OF REMOTE SENSING METHODS
TO GEOLOGIC PROBLEMS

A large part of the research done for this thesis has been concerned with the use of remote sensing methods as an aid to geologic mapping. As previously mentioned, the thesis area was selected largely on the basis of the potential it offered for testing remote sensing techniques.

Two markedly different terrains are present within the area which offer target variations in vegetation, topography, surface materials, and geology. The San Luis Valley, comprising approximately 30 percent of the thesis area, is a relatively flat expanse covered with unconsolidated Quaternary alluvial fans and alluvium. The sparse vegetation consists of grass, cactus, and some shrub. The Sangre de Cristo Mountains, which constitute the rest of the area, are very rugged and consist of deformed rocks of Precambrian and Paleozoic ages, intruded by rocks of Tertiary age. The mountains are heavily forested with conifers.

Soon after an initial evaluation of available remote sensor data, it was apparent that four major types of

geologic features could be analyzed using remote sensing techniques. These are (1) alluvial fans which occur in the San Luis Valley, (2) normal faults situated in the San Luis Valley, (3) structure and lithologic discrimination of Paleozoic sedimentary rocks on the west flank of the range, and (4) large northwest trending lineaments on the east flank of the range.

Data resulting from NASA Missions 101 (August 1969) and 105 (October 1969) had been received before research was started on this thesis. The data from these two missions, as applied to geologic problems of the thesis area, are discussed in this section. Valuable data gathered during Mission 168 (June 1971), and received from NASA during August 1971, arrived too late to be included in the main body of this section. Selected aspects of Mission 168 data are presented in the section "Recent Supplementary Data--Mission 168" (p.110-117).

Description of the Test Site

Shortly after the Hayden Pass--Orient Mine area had been selected as the test site area, it was divided into three subareas. This division was based on natural topographic boundaries and the estimated relative degree to which remote sensing methods might be successfully applied to each subarea (Map 'B'--Plate II). This subdivision was made after a cursory appraisal of available remote sensor data.

San Luis Valley--Area 'A'

Area 'A' extends from San Luis Creek to the base of the Sangre de Cristo Mountains between Hayden Pass Road and the Orient Mine (Map 'B'--Plate II). This area includes all of the San Luis Valley that is situated within the thesis area and comprises about 20 square miles. The surface of the valley is covered by alluvial fan material derived from the mountains and by fluvial deposits associated with San Luis Creek.

The coalescing alluvial fans represent episodes of fan progradation with subsequent erosion and replacement by younger fans. A classification has been developed by Knepper (1972) which subdivides the alluvial fans into groups which have similar ages. By using remote sensor data, four groups of fans were easily mapped. It was found that alluvial fans of similar ages have characteristic geomorphology and vegetation associations. These features are discussed on page 41 and under the heading "Interpretation and Evaluation of Remote Sensor Data" (p. 89).

The alluvial fans are cut by northwest trending faults which form fault scarplets up to 8 feet high (Figure 16). Most of these scarps face southwest, but three fault segments with scarps facing northeast were mapped in sections 20 and 21, T. 46 N., R. 10 E. The relative movement on these three fault segments is down on the northeast, whereas



Figure 16. Eroded fault scarp in San Luis Valley.
Dashed line marks base of scarp.

the relative movement on the other faults in the valley is down on the southwest. A normal fault of large magnitude, the Sangre de Cristo fault, separates the San Luis Valley from the Sangre de Cristo Mountains. Although covered by alluvial fan material throughout most of its length, the fault trace is expressed by alignment of vegetation near Oak Springs and by offset of fan material near the base of Steel Canyon.

Most of the water that flows from the canyons of the mountains sinks into the porous and permeable fan material of the valley. The vegetation in the valley is dominated by a sparse cover of grasses and cacti which reflect the semi-arid conditions (annual rainfall averages 10 to 15 inches per year). Limited shrub growth (mostly the greasewood, Sarcobatus vermiculatus, and rabbitbrush,

Chrysothamnus ssp), is restricted to areas of relatively greater soil moisture close to the base of the mountains and along the few stream courses which manage to transport water over the alluvial-fan material. An exception to this pattern of shrub distribution occurs in the vicinity of sections 16, 17, 20, and 21, T. 46 N., R. 10 E. (Plate I), where the moisture is fault controlled. Apparently, the fault planes present a relatively impermeable barrier to ground water moving through the alluvial fan material from the mountain front to San Luis Creek. The mechanism of water impedance is not known for certain. Since the

fault scarps in this area face southwest, the barrier cannot be topographic. A "clay series" which usually occurs at depths of 50 to 130 feet (Powell, 1958) has been reported from water wells drilled in the vicinity. It is probable that one of these impermeable clay layers has been juxtaposed against permeable gravels on the northeast side of the fault (see Figure 17).

Area 'A' is considered to be the best subarea within the thesis area for successful application of remote sensing techniques.

West Flank of the Sangre de Cristo Mountains--Area 'B'

Area 'B' extends from the western base of the Sangre de Cristo Mountains to the crest of the range between Hayden Pass Road and Black Canyon (Map 'B'--Plate II). This rugged area has 3,700 feet of relief and includes approximately 18 square miles.

The rocks found in Area 'B' consist of Precambrian crystalline rocks and Paleozoic sedimentary rocks. The Precambrian rocks are exposed in a strip along the western-most side of the mountains which averages about half a mile wide. The Precambrian lithologies include meta-sedimentary rocks and scattered igneous intrusions. Locally, foliation is so well developed that it is often mistaken for stratification on aerial photographs. A sequence of lower and middle Paleozoic sedimentary rocks nonconformably overlies the

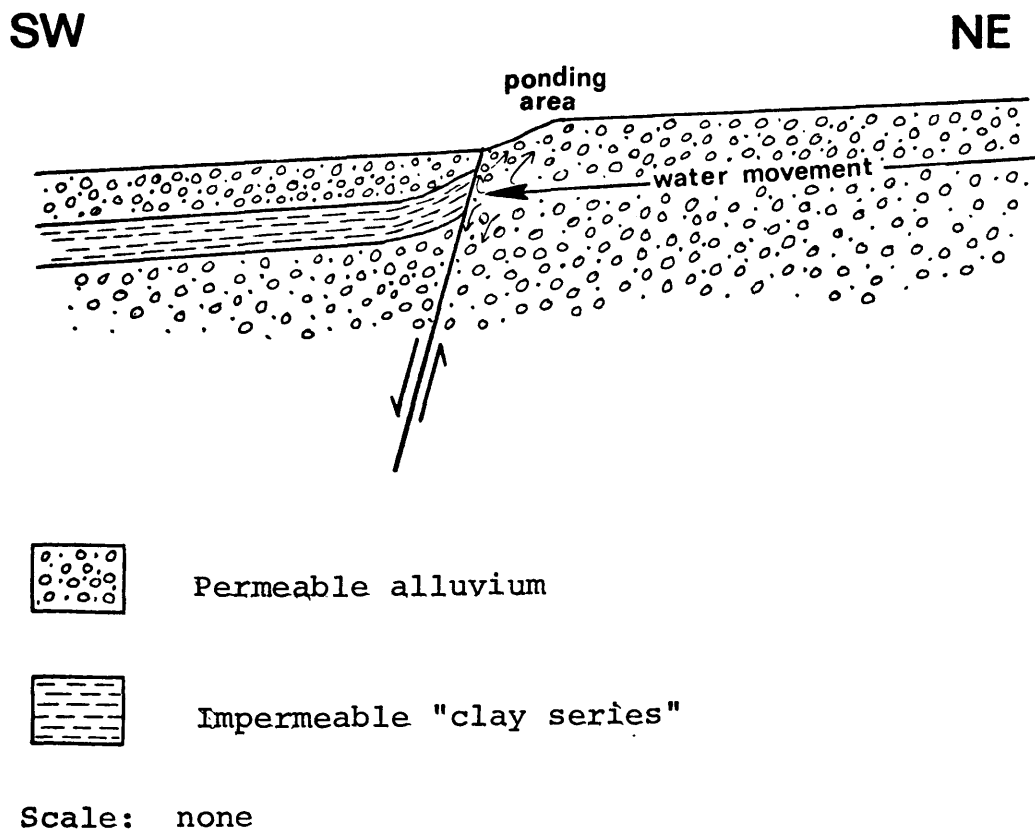


Figure 17. Hypothetical cross section of a typical fault in the San Luis Valley (Area 'A') that restricts movement of ground water and results in ponding at the surface.

Precambrian rocks and consists of relatively thin units of limestone, dolomite, and quartzite. Because of the high degree of resistance to erosion that is characteristic of these units, they are relatively well exposed. The contrasting lithologies of adjacent formations provide variations in color, vegetation, and geomorphology which facilitates discrimination and identification by remote sensing methods. Unconformably overlying the lower and middle Paleozoic rocks is a very thick sequence of upper Paleozoic clastic rocks. Some color contrast is provided by the lithologies occurring in the lower part of this sequence, but the similarities in gross lithology make differentiation of these units difficult. Only a fraction of the total upper Paleozoic section is present in Area 'B'. The rocks on the west side of the range are complexly folded and faulted.

The vegetation of Area 'B' is dominated by a thick cover of conifers. Two zones of coniferous trees are present that grade vertically into one another. The lower ponderosa pine--Douglas fir zone extends from the base of the mountains to about 9,500 feet. The spruce--fir zone extends upward from the vague upper boundary of the ponderosa pine--Douglas fir zone to timberline (approximately 11,500 feet). North-facing slopes support considerably denser stands of trees than south-facing slopes. In the valleys, and other areas of increased soil moisture,

stands of aspen are present. Triangular faceted spurs along the western base of the range, and some south-facing slopes, support scrub oak and grass. Above timberline only grasses and a few dwarfed trees exist.

Area 'B' is considered to be a moderately well suited subarea within the thesis area for successful application of remote sensing techniques.

East Flank of the Sangre de Cristo Mountains--Area 'C'

Area 'C' extends from the crest of the range to the Arkansas River between Hayden Pass Road and Big Cottonwood Creek (Map 'B'--Plate II). The area includes approximately 23 square miles of rugged terrain. Relief is on the order of 6,000 feet.

Most of Area 'C' is underlain by upper Paleozoic sedimentary rocks. In general, the lithology of these rocks is mixed conglomerates, sandstones, siltstones, and shales. Formational boundaries are based largely on differences in color. Tertiary intrusive rocks occur as dikes along the crest of the range and as a stock-like intrusion in the vicinity of Slide Rock Mountain. Near the Arkansas River, Quaternary pediment gravels and alluvium cover the surface.

Most of the sedimentary rocks of Area 'C' are folded in a regular manner. An important set of northwest trending faults were detected on small scale photography. Field evidence in support of these structures is often

minimal. It appears that three of these faults may have been significant to the emplacement of the Slide Rock Mountain Intrusive (see Plate I).

Area 'C' supports a very dense forest of conifers. The same vertical zonation of tree types exists as in Area 'B'. Because of the high density of coniferous growth, rocks are rarely seen on aerial photographs. Some of the southern facing slopes are relatively free of conifers but are usually well covered by scrub oak. A few deciduous trees grow in the lower areas near the Arkansas River. Many areas underlain by pediment gravels or alluvium are cultivated.

Of the three subareas discussed, Area 'C' is considered the least satisfactory for successful application of remote sensing methods.

Data Collection

Variables involved with the collection of remote sensor data are discussed in this section. A table is presented for each data-producing mission that summarizes important system and data parameters. Only data that concern the thesis area are considered.

Table 2. NASA Convair 990 Radar Flight--Flown May 19, 1969

<u>Mode</u>	<u>System</u>	<u>Freq.</u>	<u>Format</u>	<u>Scale</u> <u>(approx.)</u>	<u>Coverage</u>	<u>General</u> <u>Quality</u>
SLAR	Venus Fly-by	1.2 GHz	5" wide prints	1:87,000 to 1:118,000	Most of thesis area	Fair

NASA Convair 990 Radar Flight

Table 2 summarizes parameters of the Venus Fly-by radar data. Two lines of side-looking radar were flown by the NASA-Ames Convair 990 aircraft. The coverage was obtained as part of a test for the Venus Fly-by radar system. The system's 1.2 GHz center frequency provides a relatively long wavelength of 25 cm. The two northwest trending strips were flown at an altitude of 29,000 feet. The western-most strip 'looks' east at portions of the San Luis Valley and Sangre de Cristo Mountains starting from Black Canyon and continuing into the Upper Arkansas Valley. The average scale of this slant range imagery is: range scale, 1:97,500; azimuth scale, 1:87,000. The eastern strip looks west and covers portions of the Sangre de Cristo range north of Cottonwood Creek. The average scale for this strip is: range scale, 1:95,000; azimuth scale, 1:118,000. The geometric quality of the imagery, as reflected by differences in azimuth and range scales, is better on the western strip. The resolution of this radar imagery is very coarse.

NASA Mission 101

Mission 101 was flown at approximately 60,000 feet above sea level using a NASA RB-57 aircraft. Table 3 summarizes parameters of Mission 101 data. Color, color IR, and three bands of multiband photography were obtained. Stereo color transparencies (and black and white prints made from the transparencies) were obtained from an RC-8 camera with 6-inch focal length lens. An identical camera, triggered synchronously, was used to get comparative stereo color IR transparencies. A third camera, a Zeiss RMK A 30/23 with 12-inch focal length lens, was also used with color IR film. Since the scale of the Zeiss photography was twice as large as the RC-8 photography, stereo coverage was not obtained with this camera.

Multiband photography was obtained with three Hasselblad 70mm cameras equipped with 3-inch focal length lenses. All three cameras were tripped simultaneously to give comparable frame coverage. The resulting photography is of extremely small scale. The 700-900nm bandpass is seriously degraded by static discharge marks and streaking. Cloud loss is significant in several frames.

NASA Mission 105

The NASA 927-NP3A aircraft, flying at 17,500 and 25,000 feet above sea level, was used for Mission 105. Table 4 summarizes the parameters of Mission 105 data. Only a

Table 3. NASA Mission 101--Flown August 11-12, 1969

<u>Mode</u>	<u>System</u>	<u>Bandwidth</u>	<u>Film Filter</u>	<u>Format</u>	<u>Scale (Approx.)</u>	<u>Coverage</u>	<u>General Quality</u>
Photography	Wilde RC-8	400-700nm	2448	9"x9" (T) & B/W(P)	1:100,000	Entire thesis area	Excellent (few clouds)
Photography	Wilde RC-8	520-900nm	$\frac{SO-117}{W-15}$	9"x9" (T)	1:100,000	Entire thesis area	Excellent (few clouds)
Photography	Zeiss RMK A 30/23	500-900nm (approx.)	$\frac{SO-117}{Zeiss 'B'}$	9"x9" (T)	1:50,000	Most of area except just east of mtn. crest	Excellent (few clouds)
Photography (Multiband)	Hasselblad	480-590nm	$\frac{2402}{W-57}$	70mm (T)	1:200,000	All of Area 'A', Fair parts of Areas 'B' & 'C'	Fair to Good
Photography (Multiband)	Hasselblad	590-700nm	$\frac{2402}{W-25A}$	70mm (T)	1:200,000	All of Area 'A', Fair parts of Areas 'B' & 'C'	Fair to Good
Photography (Multiband)	Hasselblad	700-900nm	$\frac{SO-246}{W-89B}$	70mm (T)	1:200,000	All of Area 'A', Poor parts of Areas 'B' & 'C'	Poor

NOTE: Photography bandwidths calculated by using the 10 percent transmittance value point on Wratten filters and assuming that the responses of 2402 film and SO-246 film extend to 700nm and 900nm respectively. W = Wratten; (T) = Transparencies; (P) = Prints

Table 4. NASA Mission 105--Flown October 2, 1969.

<u>Mode</u>	<u>System</u>	<u>Bandwidth (or Freq.)</u>	<u>Film Filter</u>	<u>Format</u>	<u>Scale (Approx.)</u>	<u>Coverage</u>	<u>General Quality</u>
Photography (Color)	Wilde RC-8	400-700nm	SO-397 Anti-Vignetting	9"x9" (T&P)	1:15,000	Area 'A'; Parts of Area 'B'	Good
Photography (Color IR)	Wilde RC-8	520-900nm	SO-117 W-15 CC-20M 4600	9"x9" (T)	1:15,000	Area 'A'; Parts of Area 'B'	Poor
Photography (Multiband)	KA-62A	A 590-700nm	2402 W-25A	5"x5" (T)	1:41,000	Area 'A'; Part of Area 'B' near base of range Small part of Area 'C'	Fair
Photography (Multiband)	KA-62B	B 400-470nm	2402 W-47B	5"x5" (T)	1:41,000	"	Fair
Photography (Multiband)	KA-62C	C 500-580nm	2402 W-58	5"x5" (T)	1:41,000	"	Fair
Photography (Multiband)	KA-62D	D 700-900nm	SO-246 W-89B	5"x5" (T)	1:41,000	"	Fair
IR Scanner	RS-14	3-5.5 μ m	NA	2.5" wide strip positive (T)	L36 1:46,000	All of Area 'A'; Part of Area 'B' near base of range. Small part of Area 'C'	Fair to Good
IR Scanner	RS-14	8-14 μ m	NA	2.5" wide strip positive (T)	1:46,000	"	Good
SLAR	DPD-2	16.5 GHz	NA	2" wide strip positive (T)	1:300,000	Areas 'A' & 'B'	Very Poor
Multifrequency Microwave Radiometry	None Given	1.4 GHz 10.625 GHz 22.235 GHz 22.355 GHz 31.4 GHz	NA	Analog Magnetic Tape	NA	One line near base of moun- tains in San Luis Valley	Very Poor

NOTE: Photography bandwidths calculated by using the 10 percent transmittance value point on Wratten filters and assuming that the response of 2402 film and SO-246 film extends to 700nm and 900nm respectively. W = Wratten; (T) = Transparencies; (P) = Prints

fraction of Mission 105 objectives were accomplished due to poor weather and technical problems which resulted in unflown data lines and much unusable data.

Large scale color photography was obtained using an RC-8 camera fitted with an anti-vignetting filter. The resulting photography was of generally good quality except for some exposure problems. One side of the photographs tended to be darker than the other side. This differential darkening, which is more prominent in areas of high relief, is probably a function of the low sun angle which existed when the mission was flown. One line, which was flown in Area 'C', was too dark to use. This underexposure was probably the result of the very dense cover of conifers which have a low albedo. Stereo coverage is good in Area 'A' but marginal in Area 'B' and nonexistent in Area 'C'. The poor stereo viewing geometry is the result of severe crab used by the aircraft in order to counter strong crosswinds. The color IR has the same geometry problems and, in addition, is considerably underexposed. The color IR photography has an overall green color with some red occurring only where very abundant, healthy, nonconiferous vegetation was photographed. The color IR photography also suffers from vignetting and poor focus.

Four KA-62 cameras employing 3-inch focal length lenses were used to obtain multiband photography. The quality of the KA-62 photography was degraded by lack of good registration.

An RS-14 thermal IR scanner, recording in both the 3-5.5 μ m and 8-14 μ m bandwidths, was flown over Area 'A' and parts of Area 'B'. This imagery was obtained from about 12:11 hrs. to 13:10 hrs. Pre-dawn imagery could not be obtained due to poor weather conditions. Most of the transparencies, which were prepared from the magnetic tape output of the scanner by NASA, are of good quality. However, the 3-5.5 μ m band imagery is quite "liney" and some areas of coverage, particularly the mountainous regions, are underexposed. As received from NASA, much of the imagery was mislabeled as to which of the two channels produced it (see Lee, 1971, p. 14-15). Detracting somewhat from the comparative value of the two channels is the fact that they are not in register and are of slightly different scales.

Five lines of SLAR were flown on Mission 105. One line, which covers the west side of the northern Sangre de Cristo Range and parts of the San Luis Valley, involves the thesis area. This imagery is extremely noisy, has poor resolution, and is of very small scale. One line of multifrequency microwave radiometer data was obtained near the base of the mountains in the San Luis Valley. The data were very noisy, poorly calibrated, and lacked boresight camera reference data.

Before, during, and after the flying of Mission 105, geologists from Colorado School of Mines and Martin Marietta Corporation monitored surface and micrometeorological variables.

These variables included: cloud type and cover, wind speed and direction, relative humidity, air temperatures, radiometric (8-14 μ m and L-band) temperatures, and contact (thermister) temperatures. In addition, soil samples were collected and soil moisture content measured from these samples.

NASA Mission 115, scheduled for December 3, 1969, was postponed due to instrument malfunctions then cancelled because of adverse weather. Mission 153 (October 13-27, 1970) was also cancelled because of poor weather conditions, however, some photography was obtained outside the thesis area. Mission 168 (June 14-16, 1971) provided much useful data concerning the thesis area. These data are discussed on p. 109-116.

Interpretation and Evaluation of Remote Sensor Data

This section discusses research activities involved with the interpretation and evaluation of remote sensor data. The data are grouped according to the NASA mission that generated them. This section is introduced by a discussion of the schedule and methods used in evaluation of the data.

Schedule and Method

Dividing the thesis area into three subareas facilitated the integration of lab work and field work on a schedule that

would provide a more meaningful evaluation of remote sensor data. The general plan was to interpret the data, having little or no a priori knowledge of the area. First, a geologic map based on interpretation of the remote sensor data (Plate II) was prepared. Then a second map (Plate I) was prepared based on field observations in combination with the information available through remote sensing. Comparison of the two maps provides one indication of the usefulness and reliability of the remote sensor data.

Laboratory methods consisted of studying transparencies of the Missions 101 and 105 photography and imagery on a light table. Stereo viewing was employed where possible. The geologic interpretations were traced onto frosted mylar and then transposed to the base map using a variable scale projection technique.

The first subarea to be evaluated according to this sequence was Area 'C'. This was done because the least amount of remote sensor data was available of this area. This fact insured that interpretation could easily be completed before the 1970 summer field season began. Mission 101 color and color IR photography was studied, and several lineaments were mapped as possible faults. One line of Mission 105 photography was flown over Area 'C', but lack of stereo overlap and underexposure made these data worthless. During July and August of 1970, Area 'C' was field mapped and photogeologic features were field

checked. In preparation for the interpretation of remote sensor data of Area 'B', the formational contacts on the ridge between Silver Creek and North Piney Creek were also mapped.

During academic year 1970-71, Missions 101 and 105 remote sensor data were interpreted for Areas 'A' and 'B'. Color, color IR and multiband photography and thermal IR imagery were analyzed and geologic interpretations placed on a base map (Plate II). The previous field mapping done on the ridge between Silver Creek and North Piney Creek allowed the identification of formations and proper placement of contacts during this initial phase of mapping. Due to the complexity of structure in Area 'B' and the discontinuous exposure, considerable time was required to complete the interpretation. The alluvial fans and normal faults of the San Luis Valley, however, required less than a week of laboratory time to map. During July of 1971, subareas 'A' and 'B' were field checked and the map of Plate I was completed.

Convair 990 Radar Flight

The entire thesis area was imaged by the long wavelength, Venus Fly-by radar system. The resolution of this imagery is very coarse and only major topography is discernible. Parts of Areas 'A' and 'B', as imaged on the western-most strip of imagery, are shown in Figure 18. The break in topography between the San Luis Valley and the Sangre de Cristo Mountains

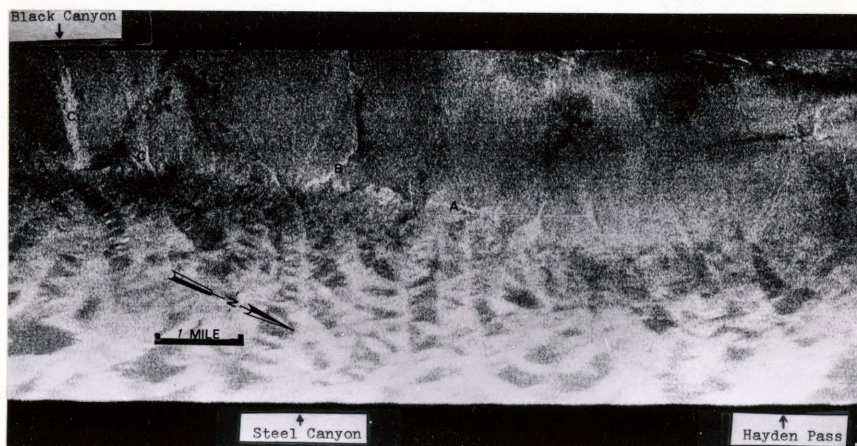


Figure 18. Reproduction of Venus Fly-by radar imagery. Radar system frequency is 1.2 GHz; look direction is to northeast; polarization is unknown.

is apparent (see feature A, Figure 18). A very high return was received from a south facing erosional scarp (approximately 50 feet high) developed in alluvial fan material northwest of Steel Canton (see feature B, Figure 18). Concentrations of shrub growth in the San Luis Valley are evident near the base of the mountains (see features C, Figure 18). The fault scarps of the San Luis Valley were not resolved by the system.

The eastern strip of imagery has lower contrast than the western strip. Even major topographic features are difficult to identify because of this low contrast.

No significant geologic data were contributed by the Convair 990 radar imagery. Radar imagery of this quality would be of very marginal value in even a more generalized regional study.

Mission 101

Mission 101 photography provided considerable aid in the selection of the Hayden Pass--Orient Mine area as a test site. The small scale (<1:100,000) allowed the viewing of large areas rapidly. In general, areas of igneous and metamorphic rock could be easily distinguished from areas of sedimentary rock. Since I was interested in working with sedimentary rocks, this helped narrow the search considerably.

Within the thesis area, rock discrimination was minimal.

In Area 'C', parts of the Tertiary intrusive could be discriminated from the surrounding sedimentary rocks (Figure 19). The small intrusive mapped in Pole Gulch on Plate I can be seen at the end of the arrow in Figure 19a. However, it was not recognized as such in the original interpretation. Precambrian terrain northeast of the Arkansas River and east of Big Cottonwood Creek was easily distinguished from the sedimentary rocks of the thesis area (Figure 19a). In Area 'B', the contact between Precambrian crystalline rocks and Paleozoic sedimentary rocks could not be accurately mapped on the small-scale photography. The strongly developed foliation of the Precambrian rocks and the thick growth of conifers contributed to this poor discrimination. The lower and middle Paleozoic rocks were easily recognized as sedimentary rocks but discrimination or identification of the thin formations was impractical with photography of such small scale. Accurate differentiation of the alluvial fans of the San Luis Valley was not possible, but some individual fans could be recognized and variations in drainage density were noticeable.

Considerable structural information was available on the Mission 101 photography. The normal faults of Area 'A' were very apparent where ponding had occurred. Some of the fault scarps could be faintly seen and mapped under high magnification. The larger folds and faults of Area 'B' were first mapped on small scale color photography. Parts of the

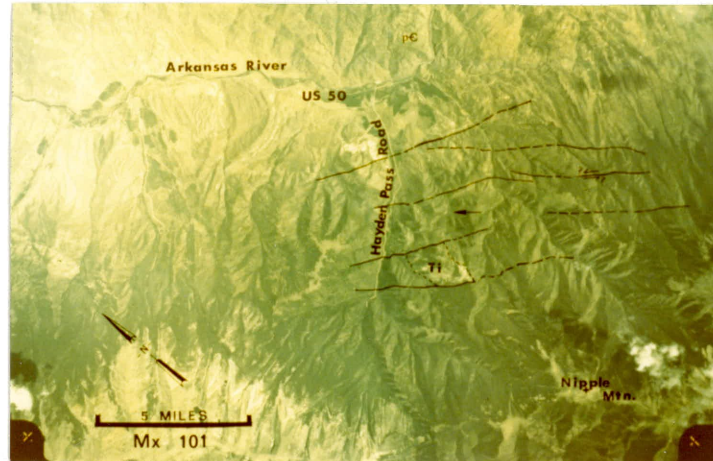


Figure 19a. Annotated reproduction of Mission 101 color photography. Area 'C' shown.

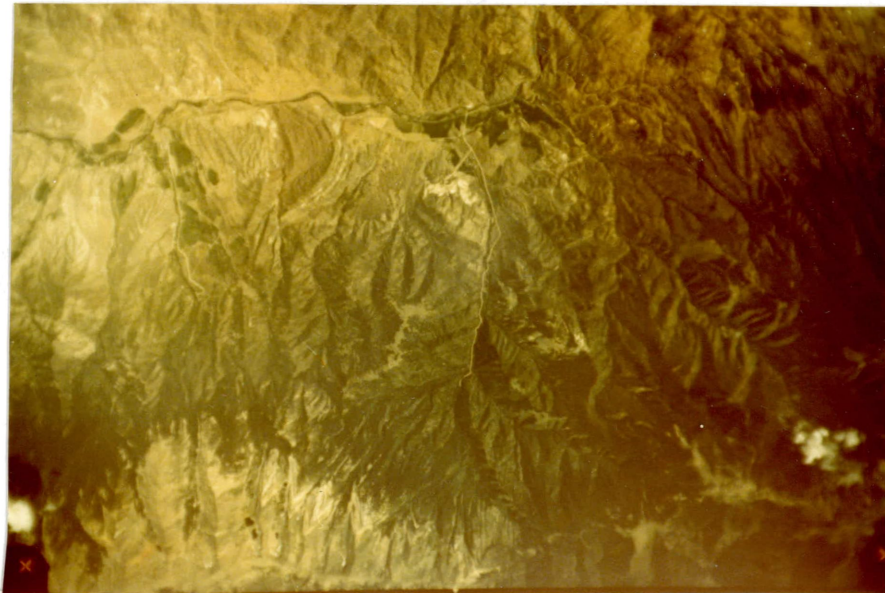


Figure 19b. Unannotated reproduction of Mission 101 color photography. Same coverage as Figure 19a.

Steel Canyon anticline and syncline, and offsets related to the Silver Creek fault, were detected (see Figure 20). The most significant structural information gleaned from Mission 101 photography was the detection and location of several northwest-trending lineaments in Area 'C' (Figure 19). These lineaments are primarily expressed topographically where small and medium scale drainage is aligned along linear trends. In some areas, these lineaments are enhanced by vegetation contrast across the lineament. In all cases except next to the Tertiary intrusive, this vegetation contrast seems to be controlled by topographic rather than lithologic control. Field evidence supports four of the five lineaments mapped from Mission 101 photography in Area 'C' (compare Plates I and II). It is significant to note that these lineaments are generally not detected on larger scale photography such as U. S. Forest Service (1:20,000 scale) black and white photography.

The difference in available information between the Mission 101 color and color IR photography is negligible. Both films did an equal job of rock discrimination. Since vegetation was significant in delineating faulting in Areas 'A' and 'C', color IR may be slightly superior in these areas. However, this advantage was judged insignificant to the final interpretation. It is interesting to note that the lineaments in Area 'C' were mapped with equal or greater ease, compared with color and color IR, on black and white contact

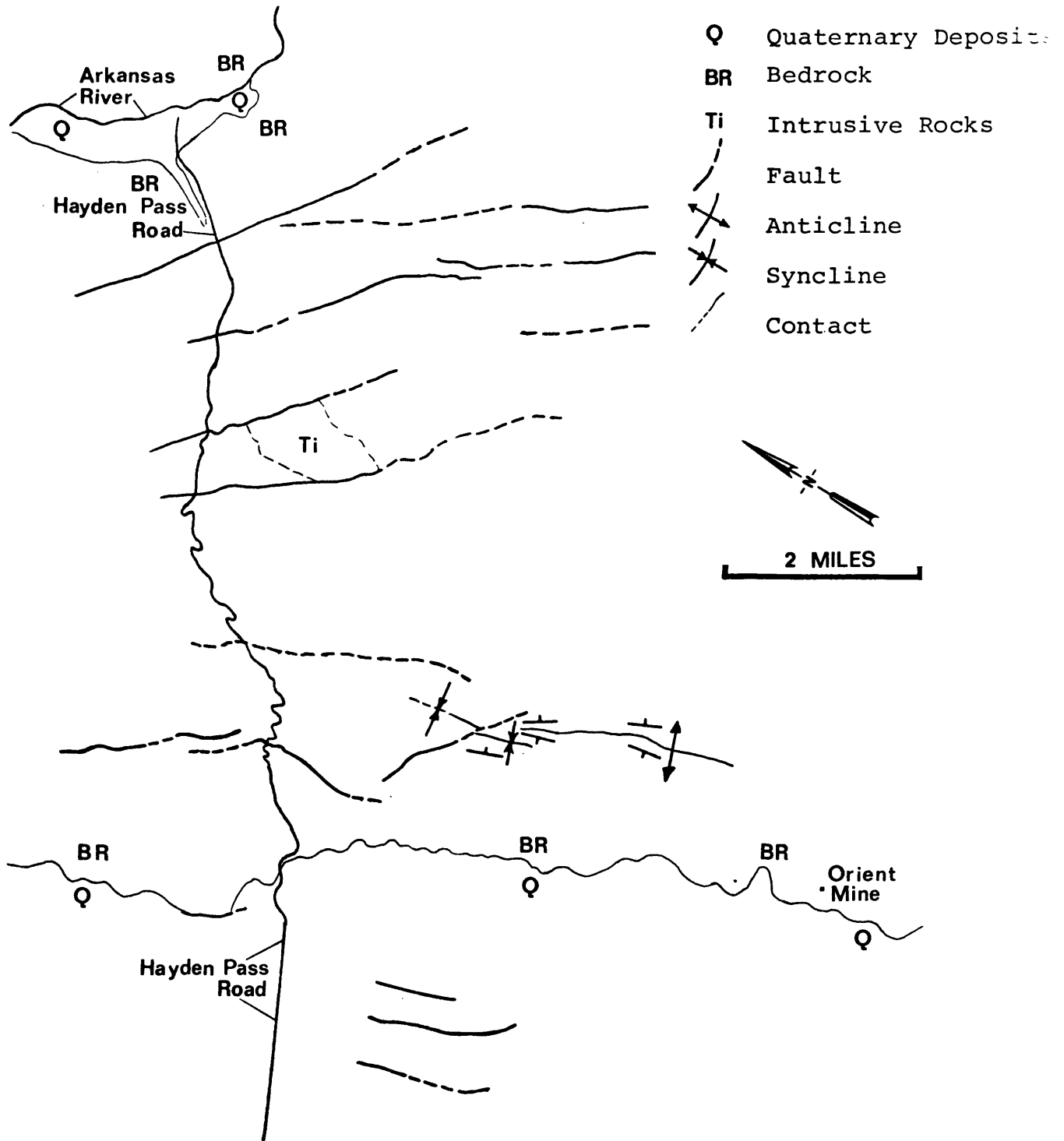


Figure 20. Geologic map based on interpretation of Mission 101 color and color IR photography.

prints made from the color transparencies. The reason for this seeming anomaly is not clear. The Zeiss color IR photography did not provide stereo viewing and was not studied in detail. However, it was obvious that some linear features, such as the fault traces of Area 'A', could be extended somewhat beyond what could be done with the Mission 101 RC-8 photography. This was entirely due to the more favorable scale and resolution of the Zeiss photography.

The multiband photography was of too small a scale to be used for anything but a more generalized regional study. Comparison of the three bandpasses is meaningless due to the high degree of variation in quality between the data. No additional information was available from the multiband photography that was not available on the color and color IR RC-8 photography.

Mission 105

The RC-8 color photography of Mission 105 was of large enough scale to provide for interpretation of detailed geology. Overall, this photography provided more useable geologic information than all the other modes of remote sensing combined. The geology of Areas 'A' and 'B' of Plate II was compiled based on interpretation of these data.

In Area 'A', the alluvial fans could be discriminated and identified. Figure 21 shows annotated and unannotated reproductions of Mission 105 color frame number 6252. On



Figure 21a. Annotated reproduction of Mission 105 color photograph. Portion of Area 'A' shown. Qmf = mud flow; Qal = alluvium; Qaf II = fan Unit II; Qaf III = fan Unit III; Os = spring.



Figure 21b. Unannotated reproduction of Mission 105 color photograph. Same area as Figure 21a is shown.

it are representatives of two of the four alluvial fan groupings. The oldest fan unit shown, Qaf III, has a higher drainage density and is topographically higher than the younger fan unit, Qaf II. Also, note that Qaf III has a slightly higher density of shrub growth. This difference in vegetation density is more apparent near the base of the mountains. Although it may not be noticeable in Figure 21 without stereo viewing, the surface of Qaf II is more gently sloped than that of Qaf III. Small erosional remnants of fan unit Qaf III have been mapped that are surrounded by Qaf II (Figure 21). These remnants of fan unit Qaf III are recognized on the photography by lighter tones and higher elevation than the surrounding Qaf II material. When later observed in the field, a relief of over 10 feet was apparent between the surfaces of the old fan remnants and the surface of the surrounding younger fan. The lighter tone of the erosional remnant surfaces is a result of the winnowing of fine material from these higher areas. This process leaves coarser material, much of which is caliche covered, exposed at the surface. As further evidence of the age relationship of the two fan units, observe that the distributaries of fan Qaf III are truncated by Qaf II. Similar criteria, which can be observed on Mission 105 color photography, are used to differentiate, identify, and correlate the other fan units of Area 'A' (see discussion on p. 41-42).

Another surface material unit has been differentiated in Figure 21 based on surface pattern and texture. This unit, designated Qmf, was interpreted to be a mud flow in which the material became supersaturated with water and flowed as a unit. The flow-like pattern of the surface strongly suggested this genesis. Field observations of these features, conducted during July of 1971, did not support this interpretation. The lighter colored areas are slightly higher than the darker areas and are covered with rock debris that is both caliche-covered and of generally light colored lithologies. In addition, these higher areas display a relatively sparse cover of grass. The anomalous pattern then, appears to be the result of the winnowing of fine material from the higher areas and the deposition of this material in the adjoining low areas. In addition to covering coarse rock debris in the lower areas, this fine material provides a more favorable substrate for grass.

Figure 21 also shows several of the fault traces of Area 'A' that are expressed as low relief scarps. The fault segments labeled a-a', b-b', c-c', d-d', and e-e' are impeding the flow of subsurface water that is moving from east to west (see discussion, p. 77-78 and Figure 17, p. 79). The resulting increase in relative soil moisture has caused an anomalously high density of vegetation on the east side of the faults. Although stereo viewing is necessary to accurately map the fault traces which are not damming

subsurface water, many of these features can be seen without the aid of stereo because of the differences in vegetation, soil, and lighting associated with the scarp slope.

Except for the postulated mud-flow features, field checks have supported all of the interpretations made in Area 'A' that were based on Mission 105 color photography. It was realized while making the field checks that compiling a geologic map of equal accuracy and completeness of Area 'A' by field mapping methods would be impractical, if not impossible.

In Area 'B', the large scale color photography is of lesser quality. The resolution of some frames is poorer and, because of dense stands of conifers, underexposure is common. The underexposure problem is amplified on north slopes because of low sun-angle and high relief. Excess aircraft yaw, used to compensate for cross winds during the overflight, resulted in a geometry which makes stereo viewing difficult. However, the large scale and good color rendition of the photography provided enough information to compile a fairly detailed geologic map of this area (see Plate II).

As previously mentioned, formational contacts were field mapped on the ridge between North Piney and Silver Creeks before laboratory interpretation began. This provided some familiarity with the lithologies and thicknesses of the formations. By later comparison of the field

mapped contacts with the color photographs, the signature characteristics of each formation and the formation boundaries were established. During interpretation, instead of merely discriminating different lithologic units and identifying these as shale, sandstone, limestone, etc., formational contacts and formational names could be applied.

The following table (Table 5) summarizes the formational characteristics that are evident on the color photography and are the basis for discrimination and identification of the rock units of Area 'B'.

Faults of Area 'B' were mapped largely on the basis of truncated or offset strata. It was noted that aspen often prefer to grow on fault zones (increased soil moisture?). The autumn photography displayed the aspen in high contrast with the conifers.

Comparison of Area 'B' on Plate I (field checked) and Plate II (interpretation of remote sensor data) reveals several discrepancies. The number of, and placement of, faults varies between the two maps, especially in the Steel Canyon area. In the vicinity of Steel Canyon, the rocks are complexly folded and faulted. The map of Plate I represents the best interpretation of data collected in the field in combination with information available from Mission 105 photography. Much more study of this area would be required to gain a full understanding of the complex structure.

Table 5. Formational characteristics of Paleozoic and Precambrian rocks of Area 'B' that are apparent on Mission 105 color photography.

Kerber Formation (Pk)	Less resistant; no outcrops, many trees.
Leadville Limestone (Ml)	Very resistant; high topography; light color; few trees; usually well exposed.
Chaffee Formation (Dc)	Characteristic yellow color; often tree covered; less resistant than Ml or Of. Contact between Dc and Of difficult to place--often based on thickness.
Fremont Dolomite (Of)	More resistant than Dc.
Harding Sandstone (Oh)	Very resistant; forms higher topography; fewer trees; notably stratified; source of many talus screes. Contact often covered by talus of Oh.
Manitou Dolomite (Om)	Less resistant than Oh; yellowish color, thickness important. Contact usually placed based on thickness of Om.
Precambrian (pE)	Similar resistance to Om; strong foliation but usually not at same attitude as bedding of adjacent sedimentary rocks, talus screes similar to Oh.

The two longitudinal faults of Plate I, which start in Black Canyon and end in Steel Canyon, were only partly detectable on the color photography where strata were offset or terminated. In the field, placement of these faults is based largely on anomalous stratigraphic thickness. The transverse fault mapped between North and South Piney creeks was misplaced on its eastern end on Plate II. Field checking of this feature revealed that brecciation and subsequent silicification of the Kerber Formation (a quartzose sandstone) had made it much more resistant than it normally is. As a result, it appeared similar to the resistant Leadville Limestone on the color photography, which led to the erroneous fault placement. In one area, on the ridge between Black and Lime canyons, so little geological information was available on the photography that it was left blank on Plate II.

The color IR photography of Mission 105 is of little value because of the overall greenish color. This is unfortunate, because the large scale of the photography would have made possible the detailed comparison of the relative usefulness of color and color IR films as applied to the geologic problems of the thesis area.

Mission 105 produced four bands of multiband photography. This photography is of adequate scale and quality to resolve many geologic features of the thesis area. The photography produced from all four film-filter combinations was examined

simultaneously on a light table. Lack of time prevented the use of more sophisticated methods of data enhancement, such as masking and color additive viewing. As is the case with Mission 101 multiband photography, it appears that no significant additional information is available from the multiband photography which is not available on the RC-8 color and color IR photography. It should be noted that the film-filter combinations used were not designed to discriminate the rocks of the thesis area. However, it was judged that Band 'D' (700-900nm) provides a better indication of the condition of grass and deciduous vegetation than did the color IR photography since Mission 105 color IR photography was improperly filtered. Marrs (Lee, 1971, p. 44-45), commenting on similar data involving the Bonanza Mining District, stated that variations in reflectance from conifers was exhibited on Bands 'B' and 'D' (400-470nm and 700-900nm respectively). Although this variation was not detected in the thesis area, more study of these two bands directed toward isolation of this spectral variance may be warranted. Variations in reflectance from conifers may be related to the geologic materials upon which the conifers grow.

The daytime thermal IR scanner imagery produced by Mission 105 is of good quality. In the mountainous areas, topography is well defined. The 3-5.5 μ m imagery, which is of higher contrast than the 8-14 μ m imagery, is locally

underexposed resulting in loss of all information. Barren areas (grass or dirt covered) can be easily distinguished from forested areas. Because of this discrimination ability, the imagery displays stratification of sedimentary rocks close to timberline (alternating vegetation zones), delineates most of Hayden Pass Road, and is able to discriminate parts of the resistant lower and middle Paleozoic rocks where these units are barren of vegetation. Neither of the igneous dikes that are exposed along the crest of the range are discriminated. The high contrast of the 3-5.5 μ m channel imagery is an advantage on a line of imagery along the base of the mountains (Line 35) where conifers are not the dominant vegetation. The alignment of trees near Oak Springs (on the trace of the Sangre de Cristo fault) and the distribution of shrub growth on the alluvial fans is well defined on this imagery. On the two lines of imagery that include the fault scarps of the San Luis Valley (Lines 33 and 34), the "lineyness" of the 3-5.5 μ m imagery degrades image resolution to such a degree that much detail of relative temperature distributions associated with the faulting is lost. The relatively high resolution provided by the 8-14 μ m imagery reveals interesting thermal details (Figure 22) of the ponding on the fault segment labeled a-a' on Figure 21a. The fault scarp itself is warm, but in the area of ponding, two relatively cool areas are surrounded by warmer areas. The cool spots are the result of both high soil moisture

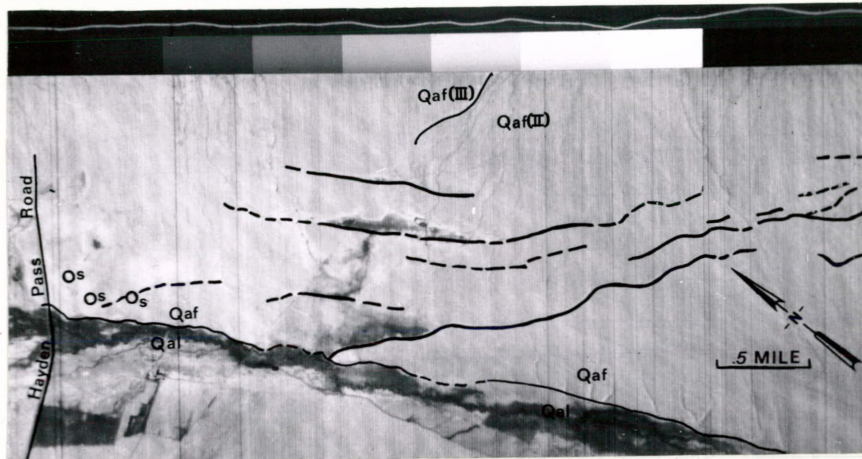


Figure 22a. Annotated reproduction of RS-14 thermal infrared scanner imagery (8-14 μ m). Qal = Quaternary alluvium; Qaf II = alluvial fan Unit II; Qaf III = alluvial fan Unit III; Os = spring. The area of ponding discussed on p. 105-106 is just below the line separating Qaf III from Qaf II at the top of the figure. Imagery taken at 1300 hours on October 2, 1969.

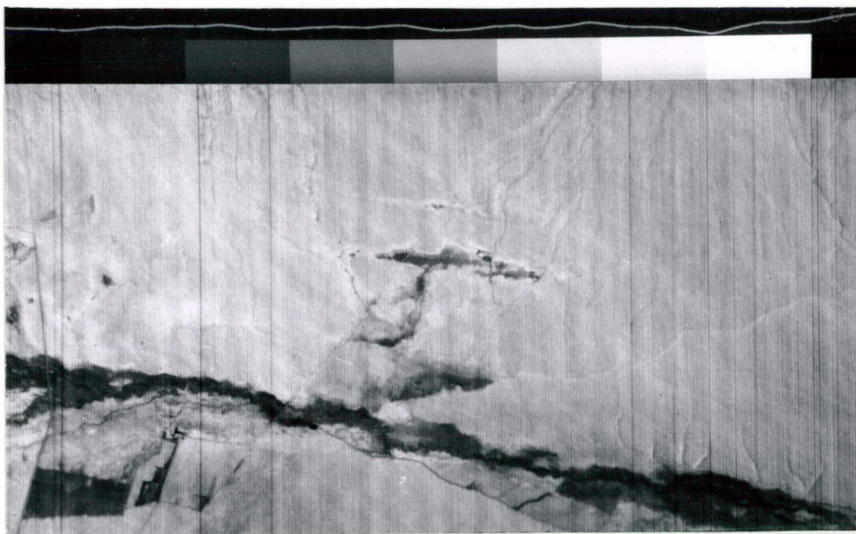


Figure 22b. Same as Figure 22a without annotations.

(evaporative cooling) and concentrations of vegetation. The relatively warm area surrounding the cool center areas might be explained by the contrasting thermal properties of the caliche material (duricrust) which is often deposited around these ponding areas. Another possible explanation would be that the slight increase in slope angle around the ponding areas may cause preferential solar heating as is the case with the fault scarps discussed below (refer to Figure 24, upper left hand corner, for close-up of picture of the area discussed). Figures 22a and 22b are annotated and unannotated reproductions of a part of Line 33. The fault scarps are imaged relatively warm as a result of topographically controlled solar heating. The scarp faces are more nearly normal to the incoming solar energy than are the adjacent areas. Note the faint streaking oriented in a north-south direction. Because of ground control operations which monitored atmospheric conditions during the overflight, these features could confidently be attributed to wind effects.

Mission 105 radar imagery was of such poor quality as to be uninterpretable. Even large topographic features were difficult or impossible to identify.

Multifrequency microwave radiometer data were analyzed by Rosecrans (Lee, 1971, p. 51) who applied several enhancement techniques to the data. His conclusion was that no geologic, hydrologic, or topographic variation produced sufficient radiometric

differences to be detected above the noise level of the radiometers. It should be noted that the microwave system was not operating properly when the data were obtained.

Recent Supplementary Data--Mission 168

Much valuable data were collected on Mission 168, which was flown during June 1971. Since these data arrived too late to be evaluated as part of this thesis, only a few highlights are discussed in this section. Table 6 summarizes the parameters of Mission 168 data that involve the thesis area.

The color and color IR photography of Mission 168 are generally superior to that produced by Mission 105. Although the scale of the Mission 168 photography is smaller, color balance, and stereo viewing geometry are superior to Mission 105 photography of the mountainous areas. Mission 105 photography of the San Luis Valley cannot be compared, since there is no comparable coverage by Mission 168 photography. Subtle color contrast between the Permo-Pennsylvanian red beds and drab, gray-green sedimentary rocks could be detected and mapped in some areas. No new structural information was apparent. The color IR provided no significant advantage in Area 'C' by virtue of the film's near IR sensitivity. Similar lithologic color contrasts were noted as with the color photography. Both color and color IR portray gypsum and limestone outcrops much more prominently than these areas are portrayed on Mission 101 and Forest Service photography.

Table 6. Summary of Remote Sensing Instrument and Data Parameters--Mission 168

<u>Mode</u>	<u>System</u>	<u>Bandwidth</u>	<u>Format</u>	<u>(Approx.) Scale</u>	<u>Coverage</u>	<u>General Quality</u>
Photography (Color)	RC-8	400-700nm	9"x9" (P & T)	1:21,000	Area 'C', small part of 'B'	Very good (Hot Spots)
Photography (Color IR)	RC-8	500-900nm	9"x9" (T)	1:21,000	Area 'C', small part of 'B'	Very good (Hot Spots)
Photography (LSAP)	RC-8	590-900nm	9"x9" (P & T)	1:33,000	All of thesis area	Excellent but flown too early in eastern area
Thermal Scanner	RS-14	8-14µm	5" strip (P & T)	1:22,000	All of Area 'A', small part of Areas 'B' & 'C'	Good
SLAR	DPD-2	16.5 GHz	2" wide strips (T)	1:360,000	All of thesis area	Poor to fair

NOTE: A small amount of multiband photography was also flown over the thesis area. Since the film/filter combinations used were not designed for discriminating the rock types of the thesis area, this photography is not discussed. LSAP = low sun-angle photography.

Low sun-angle photography (LSAP), taken during the early morning with black and white infrared film, provides excellent enhancement of the fault scarps in the San Luis Valley (Figures 23a and 23b). Black and white infrared film was used with a Wratten 25 filter to make shadows (composed mostly of scattered blue light) darker and thus increase contrast. Note the decrease in enhancement between Figure 23a and Figure 23b. The photo frame from which Figure 23b was made was exposed only 16 minutes after that of Figure 22a. During this short interval, the sun had risen sufficiently to degrade the shadow enhancement noticeably. One of the primary objectives of obtaining the LSAP was to enhance the northwest trending lineaments of Area 'C' (Reeves, 1971, p. 18). This objective was not realized. Instead of emphasizing medium and small scale drainages, which are aligned to form the lineaments, only large scale drainages are enhanced. This problem was probably the result of both the high relief of this area and the somewhat lower than optimum angle of illumination. It is apparent that different types of terrain require separate study to establish the most advantageous angle of illumination for each terrain.

Only one channel (8-14 μ m) of thermal IR scan imagery is available for analysis. During the pre-dawn overflight of the scanner, radiometric and thermometric temperatures were

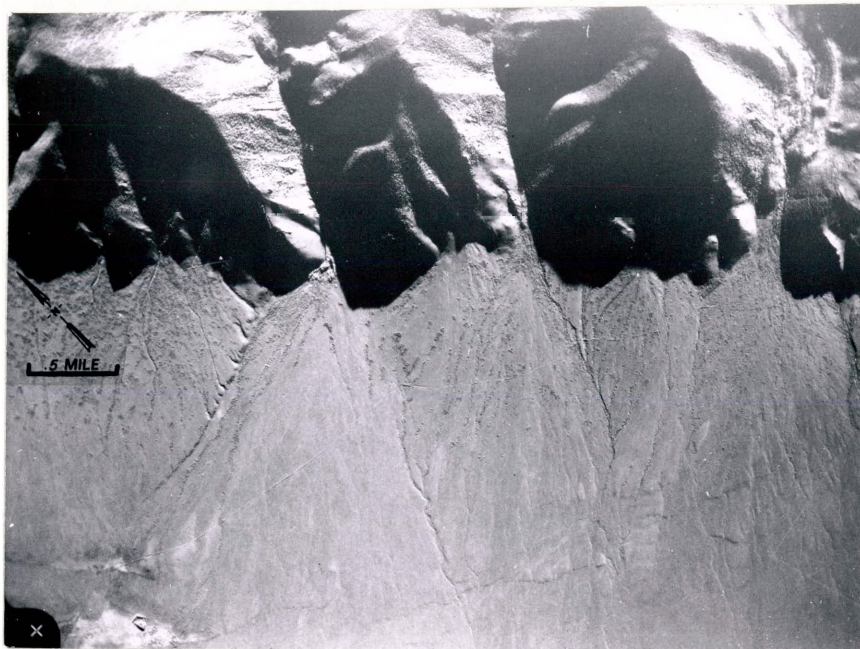


Figure 23a. LSAP of fault scarps in San Luis Valley. Note shadow enhancement. Sun-angle is approximately 24° .



Figure 23b. LSAP of same general area as Figure 23a but taken approximately 16 minutes later. Note degradation of shadow enhancement. Sun-angle is approximately 27° .

measured across a fault scarp in the San Luis Valley (Figure 24). Stations were established on the upthrown side of the fault (1), on the fault scarp (2), and on the downthrown side of the fault (3). A similar distribution of stations was established in an area where ground water ponding occurs (stations designated 'W' for 'wet') and in an adjacent area, along the same fault scarp, where no ponding occurs (stations designated 'D' for 'dry'). Figure 24 is a close-up of a U. S. Forest Service photograph showing the location of the stations. At each 'W' station, thermometric temperatures were measured at depths of 0, 2.5, 5, 10, and 20cm. At each 'D' station, temperatures were measured at 0 and 5cm depths. In addition, surface soil samples and surface radiometric temperatures (using a Barnes PRT-5) were taken at each station. Atmospheric parameters were measured at a station located between the groups of 'W' and 'D' stations. Parameters that were measured include relative humidity, wind velocity, and air temperatures at 0, 25, 50, and 100cm above the ground. The surface atmospheric data are presented in Table 7. These data suggest that evaporative cooling exerts a considerable control on relative surface temperatures. In general, radiometric temperatures are lower than corresponding thermometric temperatures, reflecting the fact that the ground surface is not a black body emitter. The imagery (Figure 25) indicates that the scanner may have a sensitivity of less than 1°C. In the area of the 'dry'

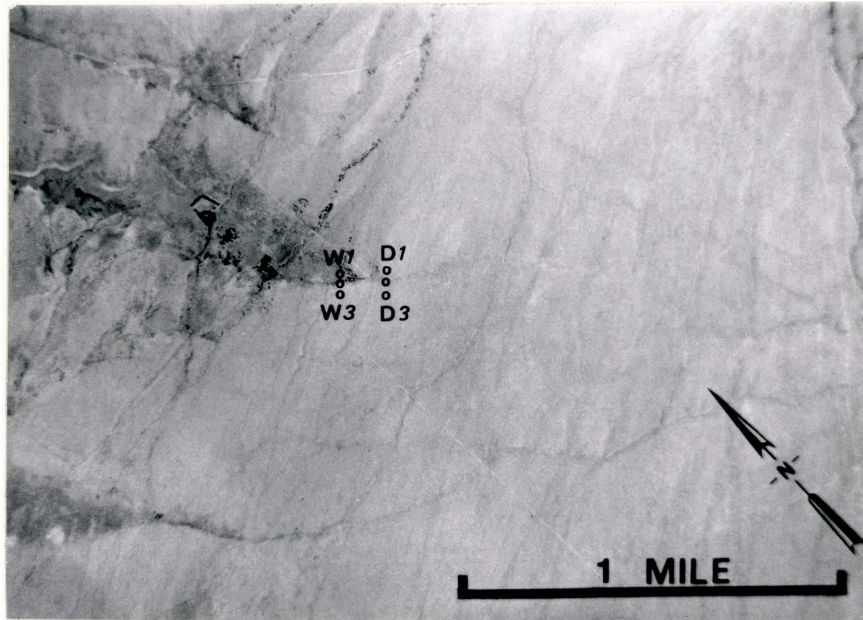


Figure 24. Close-up of Forest Service photograph showing location of temperature monitoring stations.

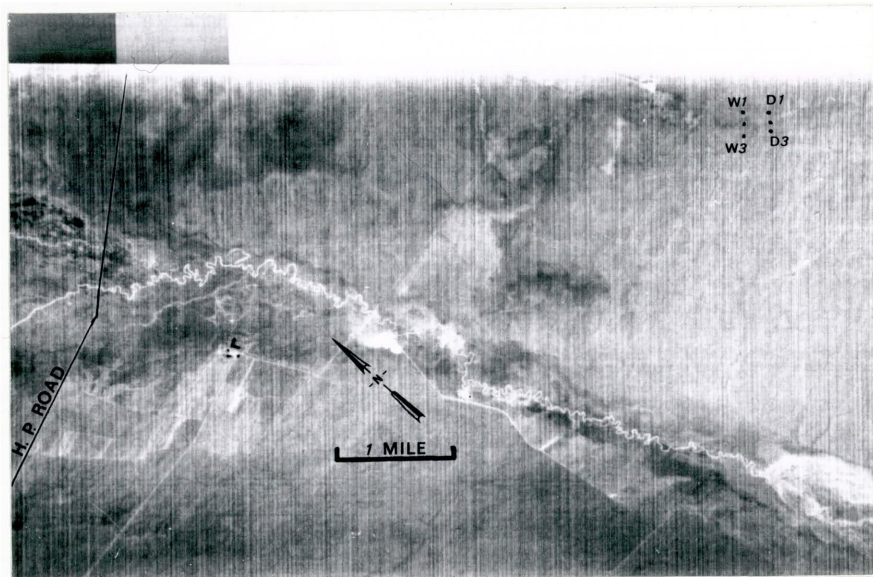


Figure 25. Reproduction of Mission 168 thermal IR imagery. Location of Hayden Pass Road and temperature monitoring stations shown. Imagery was obtained with an RS-14 in the 8-14 μ m bandwidth at 0500 hours on June 16, 1971.

Table 7. Measurements on Fault Scarps in San Luis Valley, June 16, 1971

<u>Surface Data</u>				<u>Diagrammatic Profile</u>
<u>Station</u>	<u>Surf Temp Thermomet.</u>	<u>Surf Temp Radiomet.</u>	<u>Soil Moisture</u>	
W (1)	2.3°C	2°C	2.56%	
W (2)	1.0°C	1°C	3.52%	
W (3)	3.2°C	4°C	1.99%	
D (1)	4.3°C	4°C	1.12%	
D (2)	4.6°C	4°C	1.76%	
D (3)	5.0°C	4°C	1.18%	

Atmospheric Data

<u>Air Temperature</u>			<u>Relative Humidity</u>	<u>Wind</u>
<u>Above Ground</u>	<u>Temp.</u>	<u>cm</u>		
0	2.1°C		(Dry = 43°F; Wet = 39°F)	Calm; occasional light breeze from Sangre de Cristo Mountains.
25	4.7°C			
50	5.3°C		72%	
100	5.9°C			

NOTE: Aircraft was overhead from 0440 to 0510 hours. Data are interpolated, where necessary, to this time range.

stations, the fault scarp appears relatively warm, which does not agree with the radiometric data. However, near the 'wet' stations the fault scarp is imaged relatively cool, which is consistent with surface data. Comparison between this pre-dawn imagery and Mission 105 daytime thermal imagery (Figure 22) indicates that considerably more thermal contrast is available during the day when solar heating selectively heats the scarps as a function of the slope geometry of the scarps.

The SLAR imagery of Mission 168 is superior to that of Mission 105 and the Convair 990 radar flight. However, resolution is still poor and the small scale makes it suitable only for a more generalized regional study.

Conclusions

Remote sensor data provided definite advantages in the geological evaluation of the Hayden Pass--Orient Mine area. Overall, considerable time was saved in mapping the area by applying remote sensing techniques. The geologic map resulting from the integration of remote sensor and field data is more accurate and complete than would be a map based solely on field data. In addition, a greater understanding of certain geological phenomena and the detection of geological features not previously recognized was possible by analysis of Missions 101 and 105 data.

The greatest time saving, by use of remote sensing, was

realized in Area 'A'. About 5 days of laboratory time were required to interpret the remote sensor data and transfer the interpretations to a base map. Three days were spent in the field spot-checking features of Area 'A' to confirm their identities and locations as interpreted from the remote sensor data. Except for the mud flow features (Qmf on Plate II and Figure 21a), the origin of which is not certain, the interpretations proved to be accurate. Instead of the 8 days required to map Area 'A' using remote sensing methods, the author estimates that approximately 14 days would be required to map these same 20 square miles by field methods alone.

Time savings for Area 'B' were marginal. At least 10 days were required to interpret the remote sensor data and transfer the interpretations to a base map. The complexity of the geology, the thick cover of conifers, and the poor stereo-viewing geometry of the Mission 105 photography all added to the time required for interpretation. Transferring the interpretations to the base map by using a variable scale projector was difficult because of the many scale changes needed to compensate for the high relief of Area 'B'. Ten days were required to field check Area 'B' and the author believes that more time could have been spent in the complex Steel Canyon area if additional time were available. The total of 20 days needed to map and field check Area 'B' compares

with about an equal number of days that would be required to map Area 'B' by field methods unaided by remote sensing.

In Area 'C', no significant time savings were realized by the use of remote sensing methods. This is due, in part, to the lack of remote sensor data available of this area, but more directly to the very dense cover of conifers.

Possibly more significant than the time savings made possible by using remote sensing, was the higher quality map, in terms of accuracy and completeness, that resulted from the use of remote sensor data. Based on field experience gained while spot-checking interpreted features of Area 'A', it was obvious that the alluvial fan relationships shown on Plates I and II probably would not have been recognized and, if recognized, would not have been considered as practical mapable units without remote sensor data. Many of the fault scarps in the San Luis Valley are so subtle that they would not be noticed in the field even if the presence of these features in the valley were known. In Area 'B', the Mission 105 color photography was very valuable in completing the geology between field checked control points. The color photography was also a great aid in directing field efforts to areas of complex structure or anomalous stratigraphic relationships. The northwest trending faults of Area 'C' were first detected on small-scale Mission 101 color and color IR photography. Without this photography to direct

field investigation to the specific areas of faulting, it is doubtful that all the faults would have been adequately mapped.

The method used in this thesis of evaluating a particular sensor, by comparison of a map prepared from interpretation of data from that sensor (i. e., Plate II) with a map prepared by both interpretation of remote sensor data and field data (i. e., Plate I), is beneficial but not definitive. In particular, the following factors were detrimental to a meaningful evaluation of remote sensors as applied to the thesis area:

1. Sensor data were not of consistent quality throughout the area of coverage.
2. The data were generally not of the best quality possible from the various remote sensors.
3. Complete coverage of the thesis area was not obtained by all sensors.
4. The method implies that the map supported by field data (i. e., Plate I) is correct and complete when in fact the field map is also based largely on interpretation. This is particularly true in parts of Areas 'B' and 'C'.

In addition, a more meaningful evaluation of a particular sensor could have been made if the amount of time spent interpreting the data and the amount of time spent field mapping were accurately recorded. Only general estimates can now be made for the amount of time allocated to these tasks.

The following conclusions can be made regarding the various sensor modes:

1. Color and color IR RC-8 photography provided the largest amount of valuable information. The two film types must be rated about equal in effectiveness (based on comparison of small scale Mission 101 photography and medium scale Mission 168 photography). This statement applies to the thesis area only, as previous experience has indicated that one film type may be definitely superior to the other in certain terrains. Both large and small scale photography provided valuable information and both types serve a function in the geological analysis of an area. Small scale photography provides an overall view of regional and large scale structures, and gross lithologies. It also serves to direct attention to anomalous areas deserving more study (e. g., structurally controlled ponding in the San Luis Valley). Large scale photography provides the resolution necessary to do detailed geologic mapping. The superior resolution and overall excellent quality of the Zeiss photography should be used to better advantage. Future mission planning should provide for acquisition of stereo Zeiss photography of intermediate scale for further evaluation.

2. Multiband photography was of lesser value, since the information it provided was already available on the color and color IR photography. The multiband photography would be much more competitive with the RC-8 color and color IR

photography if it were designed specifically for the rocks in the area, based on field-measured reflectance spectra, were at the same scale, and had sufficient overlap for stereo viewing. Also, multiband photography must be in register so that various enhancement techniques may be applied to the data.

3. The thermal scanner imagery proved its ability to delineate much of the faulting in the San Luis Valley, but not nearly as well as the large scale photography could. In the mountainous areas, the main control on the thermal imagery was vegetation (tree covered versus open) and topography. Direct control on surface temperatures by surface moisture content or thermal properties of rocks was not apparent. In the San Luis Valley, thermal contrast across the fault scarps is greatest during the day when solar heating is influenced by slope geometry. Pre-dawn conditions provided thermal contrasts which were of marginal magnitude to be detected by the RS-14 scanner system. Pre-dawn surface temperatures are strongly affected by soil moisture differences related to the ground water impedance along fault planes. Thermal imagery is a very specialized remote sensing tool. It can be applied most gainfully to areas of low relief and sparse vegetation that have known or suspected surface thermal contrasts. This thermal contrast can and should be established by surface temperature monitoring before data from this sensor are requested.

4. The SLAR imagery produced no useable information that was not available on small-scale photography. Although

the radar imagery that was analyzed was not of adequate quality for meaningful evaluation, some generalizations can be made. SLAR imagery is necessarily of relatively small scale and always of lesser resolution than photography of similar scale. This sensor is best suited to more generalized studies where regional structure and gross lithologic discrimination are of interest.

5. Low sun-angle photography may offer a less expensive and higher resolution alternative to SLAR imagery. In areas of contrasting relief, such as the Hayden Pass--Orient Mine area, each type of terrain must be analyzed separately in order to determine the optimum illumination-angle. In general, terrains of high relief should be photographed at higher illumination-angles than low relief terrains.

BIBLIOGRAPHY

- Atwood, W. W., and Mather, K. F., 1924, Physiographic history of the San Luis Valley of Colorado and New Mexico (abs.): Geol. Soc. Amer. Bull., Vol. 35, no. 1, p. 121-123.
- Berg, R. R., 1962, Mountain flank thrusting in Rocky Mountain foreland, Wyoming and Colorado: Am. Assoc. Petroleum Geologists Bull., v. 46, no. 11, p. 2019-2032.
- Berg, T. M., 1967, Pennsylvanian biohermal limestones of Marble Mountain, south-central Colorado: Unpublished M.Sc. thesis, Univ. of Colorado.
- Blackwelder, E., 1928, The recognition of fault scarps: Jour. Geol., v. 36, p. 289-311.
- Bolyard, D. W., 1956, Pennsylvanian and Permian stratigraphy in the Sangre de Cristo Mountains between La Veta Pass and Westcliffe, Colorado: Unpublished M.Sc. thesis, Univ. of Colorado.
- _____, 1959, Pennsylvanian and Permian stratigraphy in Sangre de Cristo Mountains between La Veta Pass and Westcliffe, Colorado: Am. Assoc. Petroleum Geologists Bull., v. 43, p. 1896-1936.
- _____, 1960, Permo-Pennsylvanian stratigraphy in the Sangre de Cristo Mountains, Colorado: Geol. Soc. America, Guide to the Geology of Colorado, p. 121-126.
- Bridwell, R. J., 1968, The geology of the Kerber Creek area, Saguache County, Colorado: Unpublished M.Sc. thesis, Colo. School Mines, 104 p.
- Briggs, L. I., and Goddard, E. N., 1956, Geology of Huerfano Park, Colo.: Rocky Mtn. Assoc. Geo., Guidebook to the Geology of the Raton Basin, p. 40-45.
- Brill, K. G., 1952, Stratigraphy of the Permo-Pennsylvanian zeugogeosyncline of Colorado and northern New Mexico: Geol. Soc. America Bull., v. 63, p. 809-880.

- Burbank, W. S., 1933, Relationship of Paleozoic and Mesozoic sedimentation to Cretaceous-Tertiary igneous activity and the development of tectonic features in Colorado; in Ore Deposits of the Western States (Lindgren volume): Am. Inst. Min. Metall. Engineers, p. 277-301.
- Burbank, W. S., and Goddard, E. N., 1937, Thrusting in Huerfano Park, Colorado, and related problems of orogeny in the Sangre de Cristo Mountains: Geol. Soc. America Bull., v. 48, p. 931-976.
- Butler, C. R., 1949, Geology of the northern part of the Sangre de Cristo Mountains, Colorado (abs.): Geol. Soc. America Bull., v. 60, no. 12, pt. 2, p. 1959-1960.
- Chapin, C. E., 1971, The Rio Grande rift, Part I: modifications and additions, in New Mexico Geol. Soc. Guidebook: 22d Field Conf., Oct., 1971, p. 191-201.
- Chronic, John, 1958, Pennsylvanian rocks in central Colorado, in Symposium on Pennsylvanian Rocks of Colorado and Adjacent Areas: Rocky Mtn. Assoc. of Geologists, p. 59-63.
- Costello, D. F., 1954, Vegetation zones in Colorado, in Harrington, H. D., Manual of the Plants of Colorado, Sage Books, Denver, p. iii-x.
- Curtis, B. F., 1958, Pennsylvanian paleotectonics of Colorado and adjacent areas, in Symposium on Pennsylvanian Rocks in Colorado and Adjacent Areas: Rocky Mtn. Assoc. Geol.
- Davis, W. M., 1913, Nomenclature of surface forms on faulted structures: Geol. Soc. America Bull., v. 24, p. 187-216.
- Dennis, J. C., (ed.), 1967, International tectonic dictionary: Am. Assoc. Petroleum Geologists Mem. 7, 196 p.
- De Voto, R. H., 1961, Geology of southwestern South Park, Park and Chaffee Counties, Colorado: Unpublished D.Sc. Thesis, Colo. School Mines, 323 p.
- _____ 1965, Pennsylvanian and Permian stratigraphy of central Colorado: The Mountain Geologist, v. 2, no. 4, p. 209-228.
- _____ 1968, Permo-Pennsylvanian block faulting and folding and the sedimentary record, central Colorado (abs.), in Geol. Soc. America Rocky Mountain Section program, p. 32.
- _____ 1971, Geologic history of South Park and geology of the Antero Reservoir quadrangle, Colorado: Colorado School Mines Quart., v. 66, no. 3, 90 p.
- _____ 1972, Permo-Pennsylvanian stratigraphy and tectonism of central Colorado: Colorado School Mines Quart., v. 67, no. 3, (in press).

- De Voto, R. H., Peel, F. A., and Pierce, W. H., 1971, Pennsylvanian and Permian stratigraphy, tectonism, and history, northern Sangre de Cristo Range, Colorado, in *New Mexico Geol. Soc. Guidebook: 22nd Field Conf., Oct., 1971*, p. 141-163.
- Endlich, F. M., 1874, Report on the mining districts of Colorado and on the geology of the San Luis district: U. S. Geol. Survey of Colo. and Adjacent territories (Hayden), Annual Report 7, p. 275-301, 305-361.
- Epis, R. C. (ed.), 1968, Cenozoic volcanism in the southern Rocky Mountains: *Colo. School Mines Quart.*, v. 63, no. 3, 287 p.
- Gabelman, J. W., 1952, Structure and origin of northern Sangre de Cristo Range, Colorado: *Am. Assoc. Petroleum Geologists Bull.*, v. 36, p. 1574-1612.
- _____, 1956, Tectonic history of the Raton Basin region: *Rocky Mtn. Assoc. Geol., Guidebook to the Geology of the Raton Basin, Colorado*, p. 35-39.
- Gaca, J. R., 1965, Gravity studies in the San Luis Valley area, Colorado: Unpublished M.Sc. Thesis, *Colo. School Mines*, 73 p.
- Gaca, J. R. and Karig, D. E., 1966, Gravity survey in the San Luis Valley area, Colorado: U. S. Geol. Survey open-file report, 21 p., 22-p app.
- Grose, L. T., 1972, Tectonics of the Rocky Mountain region: *Geologic Atlas of the Rocky Mountain Region*, Rocky Mountain Association of Geologists (in press).
- Hamilton, W. and Myers, W., 1966, Cenozoic tectonics of the Western U. S.: *Rev. Geophysics*, v. 4, p. 509-549.
- Hatfield, L. E., 1956, Stratigraphy of the Jacque Mountain and Whiskey Creek Pass Formations: M.Sc. Thesis, Unpublished, *Univ. of Colorado*, 99 p.
- Haun, J. D. and Weimer, R. J., 1960, Cretaceous stratigraphy of Colorado: *Geol. Soc. America, Guide to the Geology of Colorado*, p. 58-65.
- Haun, J. D., and Kent, H. C., 1965, Geologic history of Rocky Mountain region: *Am. Assoc. Petroleum Geologists Bull.*, v. 49, no. 11, p. 1781-1800.
- Heard, H. and Rubey, W., 1966, Tectonic implications of gypsum dehydration: *Geol. Soc. America Bull.*, v. 77, p. 741-760.

- Johnson, J. H., 1929, Contribution to the geology of the Sangre de Cristo Mountains of Colorado: Colo. Scientific Soc. Proc., v. 12, p. 1-21.
- _____ 1945, A resume of the Paleozoic stratigraphy of Colorado: Colo. School Mines Quart., v. 40, p. 1-109.
- Karig, D. E., 1964, Structural analysis of the Sangre de Cristo Range, Venable Peak to Crestone Peak, Custer and Saguache Counties, Colorado: Unpublished M.Sc. Thesis, Colo. School Mines, 143 p.
- Knepper, D. H., 1972, Tectonic evolution of the Rio Grande rift zone, central Colorado: an application of remote sensing to regional tectonic analysis: D.Sc. Thesis (in progress), Colo. School Mines.
- Koch, R. W., 1964, Geology of the Venable Peak area, Sangre de Cristo Mountains: Geol. Soc. America Bull., v. 69, p. 1143-1178
- Lee, Keenan, compiler, 1970, First annual report, NASA Grant NGL06-001-015: Dept. of Geology, Colo. School Mines.
- _____ compiler, 1971, NASA Mission 105 Summary report, NASA Grant NGL06-001-015: Dept. of Geology, Colo. School Mines.
- Litsey, L. R., 1954, Geology of the Hayden Pass--Orient area, Sangre de Cristo Mountains, Colorado: Unpublished Ph.D. dissertation, Univ. of Colorado.
- _____ 1956, Paleozoic stratigraphy of the northern Sangre de Cristo Range, Colorado, in Rocky Mtn. Assoc. Geologists Guidebook: p. 46-49.
- _____ 1958, Stratigraphy and structure of the northern Sangre de Cristo Mountains, Colorado: Geol. Soc. America Bull., v. 69, p. 1143-1178.
- _____ 1960, Geology near Orient Mine, Sangre de Cristo Mountains, Colorado, in Guide to the Geology of Colorado: Geol. Soc. America, Rocky Mtn. Assoc. Geologists, Colo. Sci. Soc., p. 129-131.
- Mallory, W. W., 1958, Pennsylvanian coarse arkosic redbeds and associated mountains in Colorado, in Symposium on Pennsylvanian rocks in Colorado and Adjacent Areas: Rocky Mtn. Assoc. Geologists, p. 17-29.
- Powell, W. J., 1958, Ground-water resources of the San Luis Valley, Colorado: U. S. Geol. Survey Water-Supply Paper 1379, 284 p.

- Mallory, W. W., 1960, Outline of Pennsylvanian stratigraphy of Colorado, in Guide to the Geology of Colorado: Geol. Soc. America, p. 23-33.
- _____ 1965, Structural geology of the Spread Eagle Peak area, Sangre de Cristo Mountains, Colorado: The Mountain Geologist, v. 2, no. 1, p. 3-21.
- Munger, R. D., 1959, Geology of the Spread Eagle Peak area, Sangre de Cristo Mountains, Colorado: Unpublished M.Sc. Thesis, Univ. of Colorado.
- NASA, 1970, Screening and indexing report, Mission 101: Earth Resources Aircraft Program.
- _____ 1970, Screening and indexing report, Mission 105: Earth Resources Program.
- Nicolaysen, G. G., 1971, Geology of the Coaldale area, Fremont County, Colorado: Unpublished M.Sc. Thesis, Colo. School Mines.
- Nolting, R. M., 1970, Pennsylvanian-Permian stratigraphy and structural geology of the Orient--Cotton Creek area, Sangre de Cristo Mountains, Colorado: Unpublished M.Sc. Thesis, Colo. School Mines.
- Oriel, S. S. and Craig, L. C., 1960, Lower Mesozoic rocks in Colorado, in Guide to the Geology of Colorado: Geol. Soc. America, p. 43-58.
- Peel, F. A., 1971, New interpretations of Pennsylvanian and Permian stratigraphy and structural history, northern Sangre de Cristo Range, Colorado: Unpublished M.Sc. Thesis, Colorado School Mines.
- Peel, F. A. and De Voto, R. H., 1972, Pennsylvanian and Permian stratigraphy and structural history of northern Sangre de Cristo Range, Colorado: Colorado School Mines Quart., v. 67, no. 3 (in press).
- Pierce, W. H., 1967, Angular unconformity within Permo-Pennsylvanian strata near Howard, Colorado (abs.), in Geol. Soc. America Rocky Mountain Section program: p. 59-60.
- _____ 1969, Geology and Pennsylvanian-Permian stratigraphy of Howard area, Fremont County, Colorado: Unpublished M.Sc. Thesis, Colo. School Mines, 136 p.

- Powers, W. E., 1935, Physiographic history of the upper Arkansas River Valley and the Royal Gorge, Colorado: Jour. Geol., v. 43, p. 184-199.
- Prucha, J. J., Graham, J. A., and Nickelsen, R. P., 1965, Basement-controlled deformation in Wyoming province of Rocky Mountains foreland: Am. Assoc. Petroleum Geologists Bull., v. 49, no. 7, p. 966-992.
- Rahman, Yousuf H., 1954, Geology of the Wellsville-Calcite area, Chaffee and Fremont Counties, Colorado: Unpublished D.Sc. dissertation, Colo. School Mines.
- Reeves, R. G., compiler, 1971, Semiannual progress report, NASA Grant NGL06-001-015: Dept. of Geology, Colo. School Mines.
- Richmond, G. M., 1960, Glaciation of the east slope of Rocky Mountain National Park, Colorado: Bull, G.S.A., v. 71, p. 1371-1382.
- Scott, G. R., 1953, Quaternary geology and geomorphic history of the Kassler Quadrangle, Colorado: U. S. Geol. Survey Prof. Paper 421-A, 70 p.
- _____ 1967, General and engineering geology of the United States Air Force Academy Site, Colorado, U.S. Geol. Survey Prof. Paper 551, 93 p.
- _____ 1970a, Quaternary faulting and potential earthquakes in east-central Colorado: U. S. Geol. Survey Prof. Paper 700-C, p. C11-C18.
- _____ 1970b, Geomorphic evolution of the southern Front Range, Colorado: Colorado Sci. Soc. unpublished Presidential Address, Dec. 21, 1970.
- Siebenthal, C. E., 1907, Notes on glaciation in the Sangre de Cristo Range: Jour. Geol., v. 15, p. 15-22.
- _____ 1910, Geology and water resources of the San Luis Valley, Colorado; U. S. Geol. Survey Water Supply Paper 240, 128 p.
- Silver, B. A., and Todd, R. G., 1969, Permian cyclic strata, northern Midland and Delaware Basins, West Texas and southeastern New Mexico: AAPG Bull., v. 53, no. 11, p. 2223-2251.

- Steven, T. A., and Epis, R. C., 1968, Ologocene volcanism in south-central Colorado: Colo. School Mines Quart., v. 63, p. 241-258.
- Stone, J. B., 1934, Limonite deposits at the Orient Mine, Colorado: Econ. Geology, v. 29, no. 4, p. 317-329.
- Stose, G. W., (ed.), 1935, Geologic map of Colorado: U. S. Geol. Survey Map.
- Toulmin, P. III, 1953, Petrography and petrology of Rito Alto Stock, Custer and Saguache Counties, Colorado: Unpublished M.Sc. Thesis, Univ. of Colorado.
- Tweto, Ogden, 1958, Pennsylvanian stratigraphic section in the Minturn-Pando area, Colorado, in Symposium on Pennsylvanian Rocks of Colorado and Adjacent Areas: Rocky Mountain Assoc. Geologists.
- Van Alstine, R. E., 1968, Tertiary trough between the Arkansas and San Luis Valleys, Colorado: U. S. Geol. Survey Prof. Paper 600-C, p. C158-C160.
- Van Alstine, R. E., and Lewis, G. E., 1960, Pliocene sediments near Salida, Chaffee County, Colorado: U. S. Geol. Survey Prof. Paper 400-B, p. B245.
- Van Andel, T. H., 1963, Recent marine sediments of Gulf of California, in Marine Geology of the Gulf of California, a Symposium: Am. Assoc. Petroleum Geologists, Memoir 3, p. 216-310.
- Vargus, D. F., 1960, Geology of the Cotopaxi inlier on the northern end of the Sangre de Cristo Range, Fremont County, Colorado: Unpublished M.Sc. Thesis, Colo. School Mines.
- Walker, T. R., 1967, Formation of redbeds in modern and ancient deserts: Geol. Soc. America Bull., v. 78, p. 353-368.



EXPLANATION

CENOZOIC	QUATERNARY	Qa1c Alluvium	Qv1c Glacial valley fill	SYMBOLS	Stippled area, arrow indicates slump
	QUATERNARY	Qa1a Alluvial fans in order of relative age. Alluvial fans of each grade have similar slope, geomorphology and vegetation characteristics. Qa1a subdivisions are of fan support.	Qm1c Mouline		Overturned anticline
PALEOZOIC	TERTIARY	T1 Undifferentiated lacustrine rocks		Overturned bedding attitude	Estimated bedding attitude
	PERMIAN	Pm1c Sangre de Cristo Formation: Lower Member		Dominant post attitude	Tectonic breccia
PALEOZOIC	PENNSYLVANIAN	Pn1c Middle Formation: limestone units (23) near top of formation		Discontinuity	Fold or fault identification letter
	PENNSYLVANIAN	Pn1b Beekmantle Formation		Discontinuity	
PALEOZOIC	MISSISSIPPIAN	Mi1c Disconformity		Discontinuity	
	DEVONIAN	Dc1c Leadville Limestone		Discontinuity	
PALEOZOIC	DEVONIAN	Dc1b Chert Formation		Discontinuity	
	DEVONIAN	Dc1a Discontinuity		Discontinuity	
PALEOZOIC	ORDOVICIAN	Or1c Fremont Gneiss		Discontinuity	
	ORDOVICIAN	Or1b Harding Sandstone		Discontinuity	
PALEOZOIC	ORDOVICIAN	Or1a Manitowish Gneiss		Discontinuity	
	ORDOVICIAN	Or1b Manitowish Gneiss		Discontinuity	
PRECAMBRIAN	Pc1c Schist, gneiss, and quartzite rocks				

1987 Magnetic North
Declination is 15°E

Scale in Miles
Base map from Harold Collins, Vado, Green, and Valley View Hill Springs USGS Quadrangles.
Cross section scale is same as map scale. 1:50,000

GEOLOGIC MAP AND CROSS SECTIONS
 HAYDEN PASS-ORIENT MINE AREA
 SAGUACHE, CUSTER, AND FREMONT COUNTIES, COLORADO
 BY
 DANIEL C. WYCHGRAM
 1972

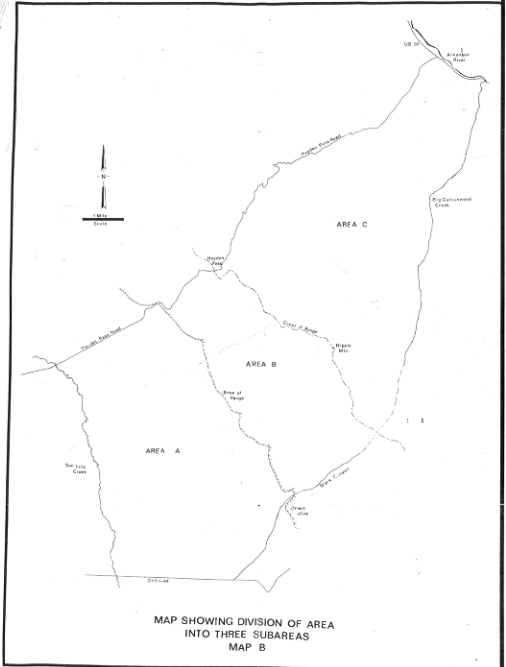
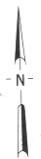


EXPLANATION

	100'		500'		1000'
<p>Map - 1:50,000 scale; 7.5-minute quadrangle Derived from aerial photography, color vegetation photographs.</p>					
	1:50,000		1:250,000		1:125,000
	1:62,500		1:31,250		1:15,625
	1:7,812		1:3,906		1:1,953
	1:976		1:488		1:244
	1:121		1:61		1:30
	1:15		1:7.5		1:3.75
	1:1.875		1:0.937		1:0.469
	1:0.234		1:0.117		1:0.059
	1:0.029		1:0.015		1:0.007

SYMBOLS

	Drainage contact (dashed where approx)
	Contact where hydrological areas were conserved
	Contact with other volcanic groups
	Additional area
	Fault, D or NW-SE, block C or NW-SE, block B
	Contact between blocks
	Contact between blocks



GEOLOGIC MAP BASED ON REMOTE SENSOR DATA—MAP A
 HAYDEN PASS—ORIENT MINE AREA
 SAGUACHE, CUSTER, AND FREMONT COUNTIES, COLORADO
 BY DANIEL C. WYCHGRAM
 1972

